Selection bias at the heterosexual HIV-1 transmission bottleneck

Jonathan M. Carlson[1*#], Malinda Schaefer[2#], Daniela C. Monaco[2], Rebecca Batorsky[3], Daniel T. Claiborne[2], Jessica Prince[2], Martin J. Deymier[2], Zachary S. Ende[2], Nichole R. Klatt[2,a], Charles E. DeZiel[1], Tien-Ho Lin[1,b], Jian Peng[1,c], Aaron M. Seese[3], Roger Shapiro[4], John Frater[5,6], Thumbi Ndung'u[3,7,8,9], Jianming Tang[10], Paul Goepfert[10], Jill Gilmour[11], Matt A. Price[12,13], William Kilembe[14], David Heckerman[15], Philip J.R. Goulder[7,16], Todd M. Allen[3], Susan Allen[14,17,18] and Eric Hunter[2*]

Affiliations:

1. Microsoft Research, Redmond, WA, USA
2. Emory Vaccine Center at Yerkes National Primate Research Center, Emory University, Atlanta, Georgia, USA
3. Ragon Institute of Massachusetts General Hospital, Massachusetts Institute of Technology and Harvard University, Cambridge, Massachusetts, USA
4. Division of Infectious Diseases, Beth Israel Deaconess Medical Center, Boston, Massachusetts, USA
5. Nuffield Department of Clinical Medicine, Oxford University, Oxford, UK
6. National Institute of Health Research, Oxford Biomedical Research Centre, Oxford, UK
7. HIV Pathogenesis Programme, Doris Duke Medical Research Institute, Nelson R. Mandela School of Medicine, University of KwaZulu-Natal, Durban, South Africa
8. KwaZulu-Natal Research Institute for Tuberculosis and HIV (K-RITH), Nelson R Mandela School of Medicine, University of KwaZulu-Natal
9. Max Planck Institute for Infection Biology, Berlin, Germany
10. Department of Medicine, University of Alabama at Birmingham (UAB), Birmingham, Alabama, USA
11. International AIDS Vaccine Initiative, London, England
12. International AIDS Vaccine Initiative, San Francisco, California, USA
13. Department of Epidemiology and Biostatistics, UCSF, SF, CA, USA
14. Zambia-Emory Research Project, Lusaka, Zambia
15. Microsoft Research, Los Angeles, California, USA
16. Department of Paediatrics, University of Oxford, Oxford, UK
17. Department of Pathology and Laboratory Medicine, Emory University, Atlanta, Georgia, USA
18. Department of Global Health, Rollins School of Public Health, Emory University, Atlanta, Georgia, USA

Current Addresses:

a. Department of Pharmaceutics, Washington National Primate Research Center, University of Washington, Seattle, WA, USA
b. Google Inc., Venice, CA, USA
c. Department of Applied Mathematics and Computer Science, Massachusetts Institute of Technology, Cambridge, MA, USA

* Correspondence to:
JMC: carlson@microsoft.com
EH: ehunte4@emory.edu

[#] Contributed equally to this manuscript

One sentence summary:

HIV transmission selects for viruses with high *in vivo* fitness, especially among males lacking genital ulcers or inflammation.

Abstract:

Heterosexual transmission of HIV-1 typically results in one genetic variant establishing systemic infection. We compared, for 137 linked transmission pairs, the amino acid sequences encoded by non-envelope genes of viruses in both partners and demonstrate a selection bias for transmission of residues that are predicted to confer increased *in vivo* fitness on viruses in the newly infected, immunologically naive recipient. Although tempered by transmission risk factors, such as donor viral load, genital inflammation, and recipient gender, this selection bias provides an overall transmission advantage for viral quasispecies that are dominated by viruses with high *in vivo* fitness. Thus, preventative or therapeutic approaches that even marginally reduce viral fitness may lower the overall transmission rates and offer long-term benefits even upon successful transmission.

SUMMARY

Introduction: Heterosexual HIV-1 transmission is an inefficient process with rates reported at <1% per unprotected sexual exposure. When transmission occurs, systemic infection is typically established by a single genetic variant, taken from the swarm of genetically distinct viruses circulating in the donor. Whether that founder virus represents a chance event or was systematically favored is unclear. Our work has tested a central hypothesis that founder virus selection is biased toward certain genetic characteristics.

Rationale: If HIV-1 transmission involves selection for viruses with certain favorable characteristics, then such advantages should emerge as statistical biases when viewed across many viral loci in many transmitting partners. We therefore identified 137 Zambian heterosexual transmission pairs, for whom plasma samples were available for both the donor and recipient partner soon after transmission, and compared the viral sequences obtained from each partner to identify features that predicted whether the majority amino acid observed at any particular position in the donor was transmitted. We focused attention on two features: viral genetic characteristics that correlate with viral fitness, and clinical factors that influence transmission. Statistical modeling indicates that the former will be favored for transmission, while the latter will nullify this relative advantage.

Results: We observed a highly significant selection bias that favors the transmission of amino acids associated with increased fitness. These features included the frequency of the amino acid in the study cohort, the relative advantage of the amino acid with respect to the stability of the protein, and features related to immune escape and compensation. This selection bias was reduced in couples with high risk of transmission. In particular, significantly less selection bias was observed in women and in men with genital inflammation, compared to healthy men, suggesting a more permissive environment in the female than male genital tract. Consistent with this observation, viruses transmitted to women were characterized by lower predicted fitness than those in men. The presence of amino acids favored during transmission predicted which individual virus within a donor was transmitted to their partner, while chronically infected individuals with viral populations characterized by a predominance of these amino acids were more likely to transmit to their partners.

Conclusion: These data highlight the clear selection biases that benefit fitter viruses during transmission in the context of a stochastic process. That such biases exist, and are tempered by certain risk factors, suggests that transmission is frequently characterized by many abortive transmission events in which some target cells are nonproductively infected. Moreover, for efficient transmission, some changes that favored survival in the transmitting partner are frequently discarded, resulting in overall slower evolution of HIV-1 in the population. Paradoxically, by increasing the selection bias at the transmission bottleneck, reduction of susceptibility may increase the expected fitness of breakthrough viruses that establish infection and may therefore worsen the prognosis for the newly infected partner. Conversely, preventative or therapeutic approaches that weaken the virus may reduce overall transmission rates via a mechanism that is independent from the quantity of circulating virus, and may therefore provide long-term benefits even upon breakthrough infection.

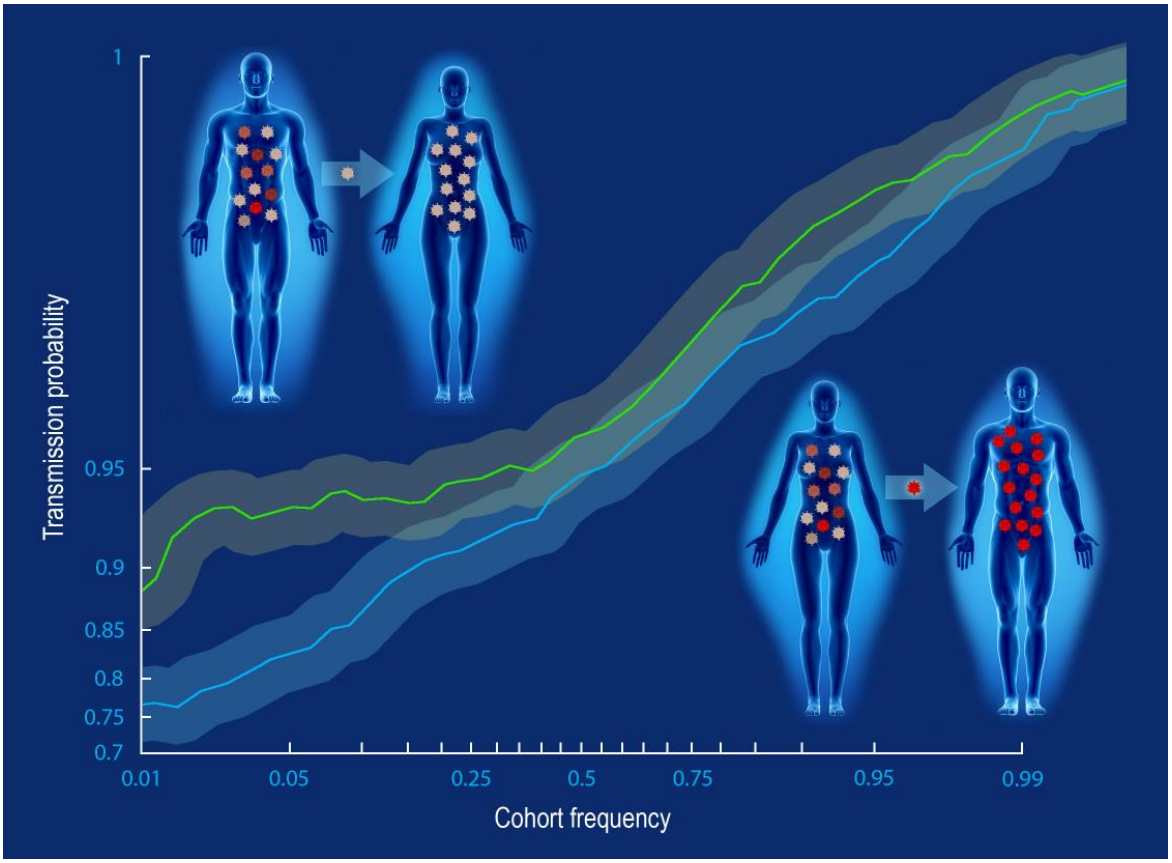

Fitter viruses (red) are favored more in woman-to-man than in man-to-woman transmission. The probability that a majority donor amino acid variant is transmitted is a function of relative fitness, here estimated by the frequency of the variant in the Zambian population. Even residues common in the population are less likely to be transmitted to healthy men than to women, indicative of higher selection bias in woman-to-man transmission.

Introduction

Heterosexual HIV-1 transmission is characterized by a severe genetic bottleneck, in which infection is typically established by a single genetic variant selected from the large and diverse quasispecies typically present in the donor (*1-7*). The source of this bottleneck is likely mediated by multiple physical and immunologic factors that limit which virus particles can reach the genital tract, penetrate the mucosal barrier, productively infect target cells, and then traffic out of the mucosa for systemic dissemination—the sum total of which effectively blocks transmission in >99% of unprotected sexual exposures (*8, 9*).

One potential source of this bottleneck is the unique environment of the male and female genital tracts, which may feature different target cell populations than those the majority of viruses face in systemic infection. The Envelope (Env) protein, expressed on the surface of virus particles, determines target cell specificity; thus variations in target cell populations are likely to exert selection pressure on the virus. Indeed, selection pressure appears to favor viruses encoding envelope proteins that utilize CCR5 as a co-receptor (*10*), that favor target cells more likely to be trafficked out of the gut (*11*), and that have higher Env concentrations (*12*). There is also evidence that envelopes with lower levels of glycosylation (*1-3, 13*) and that are closer to ancestral sequences (*14, 15*) are similarly favored. Glycosylation serves as a steric shield from the humoral immune response (*16*), while the move toward an ancestral state may involve the reversion of immunological escape mutations. Because the naïve host lacks an HIV-specific adaptive immune response, these escape features are no longer necessary and any fitness cost associated with them may become a hindrance in transmission.

If general fitness plays a role in transmission, then fitness preferences will manifest themselves in non-envelope proteins as well, the possibility of which has been recently suggested by observations that transmitted founder viruses are relatively more resistant to α-interferon (*12, 17*), a phenotype that is unlikely to be dependent on Env. The ability of virus particles to grow and efficiently infect target cells has clear pathological consequences, with *in vitro* measurements of viral replicative capacity (vRC) correlating with viral loads (VL) and CD4 decline in both acute and chronic infection (*18-21*). Importantly, VL is also closely linked with

the odds of transmission, raising the possibility that general *in vivo* viral fitness could play a significant role in the transmission process as well.

The severe nature of the transmission bottleneck suggests that the selection of the breakthrough virus is a stochastic process in which a virus with a modest growth advantage in the mucosal compartments would be more likely to succeed in establishing infection. When viewed across many linked transmission partners, such viral advantages should emerge as measurable statistical biases. We provide evidence here that the genetic bottleneck imposes a selection bias for transmission of amino acids that are consensus in the cohort and are predicted to confer increased *in vivo* fitness in the newly infected, immunologically naive recipient. This bias is tempered by transmission risk factors, such as donor viral load, genital inflammation, and recipient gender, and provides an overall transmission advantage for viral quasispecies that are dominated by viruses with high *in vivo* fitness.

Results

Consensus residues are preferentially transmitted

If some viruses with a general growth advantage are more likely to establish infection, then transmission of minority variants will be more frequent when the majority variant has lower fitness. To test this hypothesis, we collected plasma samples from 137 donors and their virologically linked seroconverting partners (recipients) a median of 46 days beyond the estimated date of infection (Table S1) and compared the amino acid variants determined by Sanger sequencing at each position in the Gag, Pol, and Nef proteins. Restricting our analysis to the 228,362 instances in which a dominant (non-mixture) residue was observed at a given position in both partners, we observed a clear bias for transmission of cohort consensus (≥50%) residues, with 99.65% of donor variants that matched cohort consensus transmitted to the partner compared with 92.61% of variants that were defined as polymorphisms (216,589 of 217,348 vs 10,200 of 11,014; $p<1e\text{-}16$, Fisher's exact test), indicating that donor minority variants are more likely to be transmitted when the donor majority variant differs from the cohort consensus. An example of this bias was observed at Nef71, which is adjacent to the critical PxxP motif implicated in SH3 domain binding and MHC Class I down regulation (*22*, *23*). Among the 114 donors where the consensus arginine was observed as the dominant donor variant, arginine was

transmitted to 112 recipients; in contrast, the dominant residue was transmitted from only 7 of 14 donors where polymorphic lysine or thronine was dominant (p=1e-6, Fisher's exact test), suggesting a bias toward the transmission of consensus arginine at this site.

Within each couple, a median of 99.69% of donor sites matching cohort consensus were transmitted, compared to only 94.38% for polymorphic donor sites (p<1e-16, sign-rank test) (Fig. 1A). Similar results were observed for sites in the donor where we observed a mixture of two amino acids in the population sequences but a single amino acid in the recipient: in these instances, consensus was still preferentially transmitted (median 60%, p=1.9e-10, sign-rank test), suggesting that this result was not driven by perfectly conserved sites that would be expected to be similarly conserved in the host (Fig. 1B).

Modeling selection bias

To further investigate the apparent bias against the transmission of non-consensus amino acids, we modeled transmission as a binomial mixture process, which assumes that each virus in the donor quasispecies is part of a subpopulation, and each virus within that subpopulation is equally and independently likely to establish infection (see methods). Assuming a low probability of transmission, the odds that a donor amino acid a at a given position is observed in the recipient founder virus F is approximately the relative frequency of a in the donor quasispecies multiplied by the relative selection advantage of a, given by

$$\frac{\Pr(a \in F)}{\Pr(a \notin F)} \approx \frac{f_a}{1-f_a} \times \frac{p_a}{p_{\overline{a}}},$$

where f_a is the frequency of viruses with a in the donor quasispecies, and $p_a/p_{\overline{a}}$ is the relative advantage for transmission that viruses with a have over viruses without a ($\overline{a}$) (p_a is the *a priori* probability that a virus of type a will establish infection, and similarly for $\overline{a}$). We refer to this latter ratio as the *selection bias* and say that the transmission bottleneck is *unbiased* if the ratio is one (i.e., if there is no selection advantage for or against a). The log of this approximation yields the following linear relationship:

$$\text{logodds}(a \in F) \approx \text{logodds}(f_a) + \text{bias}_a, \quad (1)$$

in which the log-odds that the founder virus F includes a virus with a is approximately the log-odds of the frequency of a in the donor quasispecies, shifted by the extent of selection bias

($\text{bias}_a = \log(\frac{p_a}{p_{\bar{a}}})$) for or against a. We use *increased selection bias* to refer to an increase in the absolute value of the bias, and *decreased selection bias* to mean the bias moves toward zero. The bias can be modeled as a linear function of fixed or random effects, allowing the estimation of the effects of features of interest on overall selection bias.

Confirmation of statistical model by deep sequencing

We confirmed the above relationship by deep sequencing of viruses from five linked transmission pairs, treating a as an indicator that a virus matches the donor dominant variant in the virus quasispecies at a particular site, then treating each site as an independent set of observations, to obtain sensitive estimates of the frequency of each site (f_a) in each donor. We observed a linear relationship between the log-odds of f_a and the observed log-odds of the transmission probability, with a clear bias against transmission of non-consensus polymorphisms (Fig. 2A), consistent with Eq. 1. For example, an amino acid observed in 85% of the donor viruses will be transmitted with 85% probability if it matches cohort consensus, compared to only a 65% probability if it does not.

Odds of transmission is predicted by factors related to viral fitness

Although the frequency of the amino acid in the cohort (*cohort frequency*) and in the donor's quasispecies (*quasispecies frequency*) were weakly correlated (Spearman ρ =0.18, p<1e-16; Fig S1), each was a significant predictor in a multivariable logistic regression model of transmission (p<5e-9; Table 1), consistent with cohort frequency serving as a marker of selection bias. We therefore examined the relationship between the cohort frequency of a donor amino acid and the odds of transmission in all 137 linked transmission couples and observed a strong continuous relationship between cohort frequency and transmission probability, both at sites where a mixture of amino acids was observed in the donor (Fig. 2B) and at sites where a single residue was observed (Fig. 2C). The continuous nature of these transmission/frequency curves is striking and indicates that even small changes in the relative cohort frequency of an amino acid will have a measurable effect on the odds that that amino acid will be transmitted.

Although cohort frequency is not a direct measure of *in vivo* fitness, as it may also reflect founder effects or genetic drift, it likely correlates with population-wide *in vivo* fitness. We thus

hypothesized that features that independently predict *in vivo* fitness would modulate the frequency/transmission curve. First, we found that *in silico* predicted protein stability costs of amino acid substitutions modulated the transmission curve, such that amino acids with minimal impact on the protein structure were most likely to be transmitted (Fig. 2D). Our *in silico* measure of protein stability was, by construction, biased toward consensus residues, which were most likely to match the sequence of the protein used to define the crystal structure. Nevertheless, we found that, for any given cohort frequency, an amino acid that did not impact the structure was more likely to be transmitted than an amino acid with a large impact (in the case of polymorphisms), or than a residue that occurred at a site where many other residues were equally well suited for the structure. Similarly, we found that the number of putative compensatory mutations associated with a given amino acid residue (as estimated from statistical linkage (*24*)) was correlated with an increased probability of transmission, consistent with such mutations being fixed by the compensations, or of compensatory mutations reducing the fitness cost that would otherwise be predicted by cohort frequency (Fig. 2E). Finally, sites consistent with immune escape from the donor's HLA alleles (Fig. 2F, S2A-C) were less likely to be transmitted, consistent with replicative costs frequently associated with uncompensated immune escape mutations (*18, 19, 25*). We also observed a bias against transmission of residues that could be targeted by the recipient's HLA alleles (Fig. S2D). This may suggest a selection advantage for pre-escaped viral sequences, though rapid escape and fixation after transmission could not be ruled out as an alternative cause. Differences were also observed among viral proteins (Fig. S2E and F), though such differences may primarily reflect differences in quasispecies diversity.

Each of these features was significant in a multilevel, multivariable logistic regression model (*26*) that included per-couple random effects to account for correlated regression residuals among sites taken from the same couples (Table 2). Thus, because each of these features is consistent with *in vivo* fitness, the transmission bottleneck appears to favor viruses with replicative advantages (*i.e.*, $\mathrm{bias}_a \neq 0$).

Transmission risk factors reduce selection bias

The selection bias is defined above as the *relative* ability of viruses of type a to establish infection. Some risk factors increase the odds that *any* virus will establish infection. If a risk factor increases the ability of each virus to establish infection by a constant factor *c*, as opposed to simply increasing the frequency of exposure or the viral dosage upon exposure, then the resulting selection bias is approximately $\log\frac{p_a+c}{p_{\overline{a}}+c}$, which tends toward zero as *c* becomes large relative to p_a and $p_{\overline{a}}$. Such risk factors will therefore reduce the selection bias. To test for a reduction in selection bias during transmission, we analyzed three previously reported risk factors: donor viral load (VL) (*27, 28*), male-to-female transmission (*29*), and the presence of genital ulcers or inflammation (GUI) in the recipient partners over the 12-month period prior to the event of transmission (*30, 31*). We observed a significant reduction in selection bias (most easily seen as a reduction in the effect of cohort frequency on transmission) for couples in which the donor had a high VL (Fig 3A) or the recipient was a female (Fig. 3D). Although presence of GUI had no effect on female recipients, GUI eliminated the increased selection bias experienced by male recipients (Fig. 3D). Consistent with prior observations that donor VL is a more important risk factor for male than female recipients (*27*), increased donor VL reduced the bottleneck in female-to-male (Fig. 3B), but not male-to-female (Fig. 3C), transmission, with high donor VL eliminating the increased selection bias experienced by GUI-negative male recipients (Fig. 3D-F). A composite risk index (standardized donor VL plus one if the recipient is female or a male with GUI) was significant in a multilevel, multivariable logistic regression model (p=6E-5; Table 2).

Under the assumption that the number of transmitted viruses is binomially distributed (*i.e.*, the per-virus particle probability of transmission is independent and identically distributed), the size of the donor viral population will not substantially impact selection bias (See supplementary Notes S1 and S2 and fig. S3 for a further discussion on this topic). Thus, these results suggest that the increased risk of transmission among male recipients that is linked with higher donor VL is attributable, at least in part, to increased *in vivo* viral fitness, consistent with the observation that donor VL is correlated with higher *in vitro* replicative capacity and higher early set point viral load in recipient partners (*32-34*). In contrast, the reduction in selection bias experienced by

female recipients and male recipients with GUI suggests an overall reduced selection bias, which is more conducive to infection by lower-fitness variants.

Variable reversion rates compensate for variations in selection bias

Transmission of immune escape amino acids characterized by low fitness often results in gradual reversion to high-fitness (consensus) amino acids (*35-39*), suggesting that relative reversion rates can serve as a marker for the transmission of low-fitness variants. We hypothesized that, if the selection bias acts against the transmission of less fit polymorphisms, and such bias is reduced in female recipients, then the founder viruses of women will include a higher number of costly variants, which will revert more quickly than the variants transmitted to men. We therefore collected longitudinal plasma samples for 81 of the transmission pairs at an average interval of 3 months out to 24 months post infection. Consistent with the selection bias analysis, consensus residues were transmitted at a greater proportion of polymorphic donor sites to male recipients compared to female recipients (5.98% vs 4.22%); as hypothesized, the rate at which transmitted polymorphisms reverted to consensus was significantly faster among female (0.24%/mo) than male recipients (0.12%/mo) ($p=0.016$; Fig. 4A; Fig. S4), providing further evidence that selection bias is less stringent in male to female than female to male transmission (Fig. 3D).

When we included all selection bias features in a Cox-proportional hazard model of reversion from the early founder sequences through 24 months post infection, the relative hazard of all but one feature (the structural impact of an amino acid, which had no significant effect on reversion) was consistent with what would be predicted from selection bias: selection features consistent with increased viral fitness predicted slower reversion, while selection features consistent with increased susceptibility predicted faster reversion (Table S2). In addition, recipients who were transmitted a higher number of polymorphisms at sites where the donor was polymorphic had lower early set point VL (Spearman $\rho=-0.34$, $p=0.002$; Fig. 4B), consistent with previous reports that the *in vitro gag* fitness of early viral isolates (*19, 21*), as well as transmission of HLA-B escape variants (*40, 41*), predicts early set point VL. This further corroborates the *in vivo* fitness costs of polymorphisms that are actively selected against during the transmission bottleneck and is consistent with our previous observation of a significantly lower VL in these women early in infection (*34*).

Estimating the odds of transmission of entire viral sequences and populations

The selection bias models described above result in a predicted log-odds that a given residue at a given site will be transmitted. If we treat all sites within an individual as independent (conditioned on the protein), then the mean of the predicted log-odds over a given viral sequence yields a *transmission index* that estimates how likely overall an individual sequence is to be transmitted. Given the observed selection bias, we expect that founder viruses will tend to have above-average transmission indices relative to the donor quasispecies. Using limiting dilution single genome amplification, we obtained a median of 19 (range [4, 27]) *gag* sequences for each of 17 donors and compared the transmission indices of donor amplicons to those of the linked founder sequences. Overall, founder sequences had higher than expected *gag* transmission indices (Fig. 5A-B; p=0.02), though viruses with even higher transmissibility indices were frequently observed in the donor quasispecies, highlighting the stochastic nature of transmission. The observed variation in mean donor transmissibility suggests that some quasispecies are, on average, more transmissible than others and may therefore be more likely to establish infection. To test this, we obtained *gag*, *pol* and *nef* sequences from 181 risk-matched, chronically infected individuals who had not transmitted to their partners. Overall, chronically infected partners who had transmitted exhibited higher median transmission indices than individuals who had not yet transmitted (p=0.009; Fig. 5C), an effect that remained significant when controlling for the donor VL, recipient gender, and GUI risk factors (Table S3).

Discussion

The recognition that a single virus, or at most a handful of viruses, establishes infection led to great optimism that the defining characteristics of transmitted founder viruses would be readily identified, leading to a clear vaccine strategy. Although selection bias has been observed to act upon the Env protein (*1-3, 10, 12, 42*), and may favor viruses that are relatively resistant to interferon-α (*12*), no deterministic features have yet been identified. Rather, the bottleneck appears to act at a stochastic level, favoring, though not exclusively, viruses with higher overall fitness in the context of the mucosal compartment. Here we show that selection bias also acts on non-Env proteins and can be estimated by such generic features as the effect of a variant on protein stability, dependency of the variant on compensation, and the overall frequency of the variant in the cohort. That each of these features also predicts rates of reversion in the linked

recipient further supports their role as markers of *in vivo* fitness. These observations confirm the hypothesis that minor fitness advantages play an important role in transmission beyond features that depend on the nature of target cells in the mucosa. Although the majority of these features likely correlate with fitness in many immunological compartments, the observation that variants linked to immune escape in the donor were less likely to be transmitted—and more likely to revert if they were transmitted—highlights the fact that *in vivo* fitness in chronic infection must account for immune pressures that may be absent at the site of transmission. As a result of selection bias, transmission often results in a step back in evolutionary time towards consensus, thereby slowing the rate of population-wide evolution, consistent with the low rate of population-wide evolution observed in the North American epidemic (*43*).

The observation that transmission risk factors reduce the selection bias further corroborates the role of fitness in transmission and provides important clues as to the mechanisms of increased risk. In the case of donor VL, while the quantity of virus during exposure likely plays a role in increased risk, it cannot explain the observed reduction in selection bias, suggesting that the underlying fitness typical of high VL is playing an important role as well (see supplemental note S1 for simulation experiments and a further discussion on this point). This in turn suggests that interventions that reduce VL without altering viral fitness (such as antiretroviral therapy in the absence of virologic escape) will have diminished effects on transmission compared to those that similarly reduce VL but additionally weaken the virus. Conversely, immunological escapes that confer a net advantage to the virus in the donor, and therefore result in higher VL, may nonetheless reduce the rate of transmission as a result of weakening the virus.

Selection bias was here measured by comparing genetic variants found in donor and recipient blood, and thus in principle could reflect selection occurring at any number of steps, including selection of viruses in the donor genital compartment or productive infection followed by reversion. Our previous SGA analysis of virus variants in the donor genital tract of Zambian transmission pairs argued against preferential selection in this compartment (*44*), and a deeper analysis of the reversion data also provides evidence that the selection bias observed above is not an artifact of rapid reversion in the narrow time frame of acute infection. First, non-parametric estimates of reversion rates place the rate of reversion at 0.12% per month for males (0.24% for

females), a rate that holds constant after 3 months of infection. In contrast, the inferred rate of reversion peaks during the transmission window with a maximum that is an order of magnitude higher than the constant rate observed during the remainder of the sample period (Fig S4). It is unlikely that reversion rates would change so suddenly, and phylogenetic analyses of single genome amplified viral sequences from these early time points in this cohort (*3, 6, 44*) strongly argue against the founder virus undergoing significant rapid reversion in the first few days post transmission that must be enabled by rapid selective sweeps. Moreover, the observation in this study that features that reduced selection bias predict faster reversion is not consistent with the proposition that selection bias is an artifact of rapid reversion, as it would require reversion rates to be faster in men in the first month of infection and faster in women in the following years. These data thus argue that selection bias occurs primarily at the site of transmission, and suggest that sexual exposure frequently results in non-productive infection of target cells until viruses with higher fitness gain a foothold for successful dissemination.

The observation that sequence features alone can predict the odds of transmission for a particular virus population highlights the importance of transmission selection bias and provides a clear mechanism for risk factors that reduce selection bias by increasing virulence or susceptibility. In addition, transmission of even subtly weaker viruses, either by increased susceptibility that allows transmission of less fit viruses from the donor quasispecies or because all variants in the donor quasispecies have lower fitness, may result in a clinical advantage for recipients (*40, 41*). Although the advantage of such subtle effects may be short-lived due to increased reversion that typically restore viral fitness, previous reports indicate that replicative fitness costs of early viral sequences result in a sustained clinical advantage for the linked recipient (*19, 21*). Paradoxically, by increasing the selection bias at the transmission bottleneck, reduction of susceptibility would increase the expected fitness of breakthrough viruses that manage to establish infection and may therefore worsen the prognosis for the newly infected partner. Conversely, preventative or therapeutic approaches that even marginally weaken the virus may reduce overall transmission rates via a mechanism that is independent from the quantity of circulating virus and may provide long-term benefits even upon successful transmission.

References:

1. M. R. Abrahams, J. A. Anderson, E. E. Giorgi, C. Seoighe, K. Mlisana *et al.*, Quantitating the multiplicity of infection with human immunodeficiency virus type 1 subtype C reveals a non-poisson distribution of transmitted variants. *J Virol* **83**, 3556-3567 (2009).

2. C. A. Derdeyn, J. M. Decker, F. Bibollet-Ruche, J. L. Mokili, M. Muldoon *et al.*, Envelope-constrained neutralization-sensitive HIV-1 after heterosexual transmission. *Science* **303**, 2019-2022 (2004).

3. R. E. Haaland, P. A. Hawkins, J. Salazar-Gonzalez, A. Johnson, A. Tichacek *et al.*, Inflammatory genital infections mitigate a severe genetic bottleneck in heterosexual transmission of subtype A and C HIV-1. *PLoS Pathog* **5**, e1000274 (2009).

4. B. F. Keele, E. E. Giorgi, J. F. Salazar-Gonzalez, J. M. Decker, K. T. Pham *et al.*, Identification and characterization of transmitted and early founder virus envelopes in primary HIV-1 infection. *Proc Natl Acad Sci U S A* **105**, 7552-7557 (2008).

5. B. Etemad, A. Fellows, B. Kwambana, A. Kamat, Y. Feng *et al.*, Human immunodeficiency virus type 1 V1-to-V5 envelope variants from the chronic phase of infection use CCR5 and fuse more efficiently than those from early after infection. *J Virol* **83**, 9694-9708 (2009).

6. J. F. Salazar-Gonzalez, E. Bailes, K. T. Pham, M. G. Salazar, M. B. Guffey *et al.*, Deciphering human immunodeficiency virus type 1 transmission and early envelope

diversification by single-genome amplification and sequencing. *J Virol* **82**, 3952-3970 (2008).

7. A. J. Frater, C. T. Edwards, N. McCarthy, J. Fox, H. Brown *et al.*, Passive sexual transmission of human immunodeficiency virus type 1 variants and adaptation in new hosts. *J Virol* **80**, 7226-7234 (2006).

8. G. M. Shaw, E. Hunter, HIV transmission. *Cold Spring Harbor perspectives in medicine* **2**, (2012).

9. R. A. Royce, A. Sena, W. Cates, Jr., M. S. Cohen, Sexual transmission of HIV. *N Engl J Med* **336**, 1072-1078 (1997).

10. E. A. Berger, P. M. Murphy, J. M. Farber, Chemokine receptors as HIV-1 coreceptors: roles in viral entry, tropism, and disease. *Annu Rev Immunol* **17**, 657-700 (1999).

11. C. Cicala, J. Arthos, A. S. Fauci, HIV-1 envelope, integrins and co-receptor use in mucosal transmission of HIV. *J Transl Med* **9 Suppl 1**, S2 (2011).

12. N. F. Parrish, F. Gao, H. Li, E. E. Giorgi, H. J. Barbian *et al.*, Phenotypic properties of transmitted founder HIV-1. *Proc Natl Acad Sci U S A* **110**, 6626-6633 (2013).

13. S. Gnanakaran, T. Bhattacharya, M. Daniels, B. F. Keele, P. T. Hraber *et al.*, Recurrent Signature Patterns in HIV-1 B Clade Envelope Glycoproteins Associated with either Early or Chronic Infections. *PLoS Pathog* **7**, e1002209 (2011).

14. M. Sagar, O. Laeyendecker, S. Lee, J. Gamiel, M. J. Wawer *et al.*, Selection of HIV variants with signature genotypic characteristics during heterosexual transmission. *J Infect Dis* **199**, 580-589 (2009).

15. J. T. Herbeck, D. C. Nickle, G. H. Learn, G. S. Gottlieb, M. E. Curlin *et al.*, Human immunodeficiency virus type 1 env evolves toward ancestral states upon transmission to a new host. *J Virol* **80**, 1637-1644 (2006).

16. X. Wei, J. M. Decker, S. Wang, H. Hui, J. C. Kappes *et al.*, Antibody neutralization and escape by HIV-1. *Nature* **422**, 307-312 (2003).

17. A. E. Fenton-May, O. Dibben, T. Emmerich, H. Ding, K. Pfafferott *et al.*, Relative resistance of HIV-1 founder viruses to control by interferon-alpha. *Retrovirology* **10**, 146 (2013).

18. M. A. Brockman, Z. L. Brumme, C. J. Brumme, T. Miura, J. Sela *et al.*, Early selection in Gag by protective HLA alleles contributes to reduced HIV-1 replication capacity that may be largely compensated for in chronic infection. *J Virol* **84**, 11937-11949 (2010).

19. J. L. Prince, D. T. Claiborne, J. M. Carlson, M. Schaefer, T. Yu *et al.*, Role of transmitted Gag CTL polymorphisms in defining replicative capacity and early HIV-1 pathogenesis. *PLoS Pathog* **8**, e1003041 (2012).

20. J. K. Wright, Z. L. Brumme, J. M. Carlson, D. Heckerman, C. M. Kadie *et al.*, Gag-protease-mediated replication capacity in HIV-1 subtype C chronic infection: associations with HLA type and clinical parameters. *J Virol* **84**, 10820-10831 (2010).

21. J. K. Wright, V. Novitsky, M. A. Brockman, Z. L. Brumme, C. J. Brumme *et al.*, Influence of Gag-protease-mediated replication capacity on disease progression in individuals recently infected with HIV-1 subtype C. *J Virol* **85**, 3996-4006 (2011).

22. M. E. Greenberg, A. J. Iafrate, J. Skowronski, The SH3 domain-binding surface and an acidic motif in HIV-1 Nef regulate trafficking of class I MHC complexes. *EMBO J* **17**, 2777-2789 (1998).

23. A. Mangasarian, V. Piguet, J. K. Wang, Y. L. Chen, D. Trono, Nef-induced CD4 and major histocompatibility complex class I (MHC-I) down-regulation are governed by distinct determinants: N-terminal alpha helix and proline repeat of Nef selectively regulate MHC-I trafficking. *J Virol* **73**, 1964-1973 (1999).

24. J. M. Carlson, Z. L. Brumme, C. M. Rousseau, C. J. Brumme, P. Matthews *et al.*, Phylogenetic dependency networks: inferring patterns of CTL escape and codon covariation in HIV-1 Gag. *PLoS Comput Biol* **4**, e1000225 (2008).

25. C. L. Boutwell, C. F. Rowley, M. Essex, Reduced viral replication capacity of human immunodeficiency virus type 1 subtype C caused by cytotoxic-T-lymphocyte escape mutations in HLA-B57 epitopes of capsid protein. *J Virol* **83**, 2460-2468 (2009).

26. G. Y. Wong, W. M. Mason, The Hierarchical Logistic-Regression Model for Multilevel Analysis. *J Am Stat Assoc* **80**, 513-524 (1985).

27. U. S. Fideli, S. A. Allen, R. Musonda, S. Trask, B. H. Hahn *et al.*, Virologic and immunologic determinants of heterosexual transmission of human immunodeficiency virus type 1 in Africa. *AIDS Res Hum Retroviruses* **17**, 901-910 (2001).

28. R. H. Gray, M. J. Wawer, R. Brookmeyer, N. K. Sewankambo, D. Serwadda *et al.*, Probability of HIV-1 transmission per coital act in monogamous, heterosexual, HIV-1-discordant couples in Rakai, Uganda. *Lancet* **357**, 1149-1153 (2001).

29. Comparison of female to male and male to female transmission of HIV in 563 stable couples. European Study Group on Heterosexual Transmission of HIV. *BMJ* **304**, 809-813 (1992).

30. S. R. Galvin, M. S. Cohen, The role of sexually transmitted diseases in HIV transmission. *Nat Rev Microbiol* **2**, 33-42 (2004).

31. J. Tang, W. Shao, Y. J. Yoo, I. Brill, J. Mulenga *et al.*, Human leukocyte antigen class I genotypes in relation to heterosexual HIV type 1 transmission within discordant couples. *Journal of Immunology* **181**, 2626-2635 (2008).

32. F. M. Hecht, W. Hartogensis, L. Bragg, P. Bacchetti, R. Atchison *et al.*, HIV RNA level in early infection is predicted by viral load in the transmission source. *AIDS* **24**, 941-945 (2010).

33. T. D. Hollingsworth, O. Laeyendecker, G. Shirreff, C. A. Donnelly, D. Serwadda *et al.*, HIV-1 transmitting couples have similar viral load set-points in Rakai, Uganda. *PLoS Pathog* **6**, e1000876 (2010).

34. L. Yue, H. A. Prentice, P. Farmer, W. Song, D. He *et al.*, Cumulative impact of host and viral factors on HIV-1 viral-load control during early infection. *J Virol* **87**, 708-715 (2013).

35. T. M. Allen, M. Altfeld, X. G. Yu, K. M. O'Sullivan, M. Lichterfeld *et al.*, Selection, transmission, and reversion of an antigen-processing cytotoxic T-lymphocyte escape mutation in human immunodeficiency virus type 1 infection. *J Virol* **78**, 7069-7078 (2004).

36. Z. L. Brumme, C. J. Brumme, J. Carlson, H. Streeck, M. John *et al.*, Marked epitope- and allele-specific differences in rates of mutation in human immunodeficiency type 1 (HIV-1) Gag, Pol, and Nef cytotoxic T-lymphocyte epitopes in acute/early HIV-1 infection. *J Virol* **82**, 9216-9227 (2008).

37. H. Crawford, J. G. Prado, A. Leslie, S. Hue, I. Honeyborne *et al.*, Compensatory mutation partially restores fitness and delays reversion of escape mutation within the immunodominant HLA-B*5703-restricted Gag epitope in chronic human immunodeficiency virus type 1 infection. *J Virol* **81**, 8346-8351 (2007).

38. A. Leslie, D. Kavanagh, I. Honeyborne, K. Pfafferott, C. Edwards *et al.*, Transmission and accumulation of CTL escape variants drive negative associations between HIV polymorphisms and HLA. *J Exp Med* **201**, 891-902 (2005).

39. J. Martinez-Picado, J. G. Prado, E. E. Fry, K. Pfafferott, A. Leslie *et al.*, Fitness cost of escape mutations in p24 Gag in association with control of human immunodeficiency virus type 1. *J Virol* **80**, 3617-3623 (2006).

40. D. R. Chopera, Z. Woodman, K. Mlisana, M. Mlotshwa, D. P. Martin *et al.*, Transmission of HIV-1 CTL escape variants provides HLA-mismatched recipients with a survival advantage. *PLoS Pathog* **4**, e1000033 (2008).

41. P. A. Goepfert, W. Lumm, P. Farmer, P. Matthews, A. Prendergast *et al.*, Transmission of HIV-1 Gag immune escape mutations is associated with reduced viral load in linked recipients. *J Exp Med* **205**, 1009-1017 (2008).

42. C. Cicala, E. Martinelli, J. P. McNally, D. J. Goode, R. Gopaul *et al.*, The integrin alpha4beta7 forms a complex with cell-surface CD4 and defines a T-cell subset that is highly susceptible to infection by HIV-1. *Proc Natl Acad Sci U S A* **106**, 20877-20882 (2009).

43. L. A. Cotton, X. T. Kuang, A. Q. Le, J. M. Carlson, B. Chan *et al.*, Genotypic and functional impact of HIV-1 adaptation to its host population during the North American epidemic. *PLoS Genetics* **In Press**, (2014).

44. J. F. Salazar-Gonzalez, M. G. Salazar, B. F. Keele, G. H. Learn, E. E. Giorgi *et al.*, Genetic identity, biological phenotype, and evolutionary pathways of transmitted/founder viruses in acute and early HIV-1 infection. *J Exp Med* **206**, 1273-1289 (2009).

45. B. Efron, Nonparametric standard errors and confidence intervals. *Canadian Journal of Statistics* **9**, 139-158 (1981).

46. S. Allen, E. Karita, E. Chomba, D. L. Roth, J. Telfair *et al.*, Promotion of couples' voluntary counselling and testing for HIV through influential networks in two African capital cities. *BMC Public Health* **7**, 349 (2007).

47. M. C. Kempf, S. Allen, I. Zulu, N. Kancheya, R. Stephenson *et al.*, Enrollment and retention of HIV discordant couples in Lusaka, Zambia. *J Acquir Immune Defic Syndr* **47**, 116-125 (2008).

48. S. L. McKenna, G. K. Muyinda, D. Roth, M. Mwali, N. Ng'andu *et al.*, Rapid HIV testing and counseling for voluntary testing centers in Africa. *AIDS* **11**, S103-110. (1997).

49. S. A. Trask, C. A. Derdeyn, U. Fideli, Y. Chen, S. Meleth *et al.*, Molecular epidemiology of human immunodeficiency virus type 1 transmission in a heterosexual cohort of discordant couples in Zambia. *J Virol* **76**, 397-405 (2002).

50. V. Piguet, D. Trono, in *Human Retroviruses and AIDS 1999*, C. L. Kuiken *et al.*, Eds. (Theoretical Biology and Biophysics Group, Los Alamos National Laboratory, Los Alamos, NM., Los Alamos, NM., 1999), pp. 448-459.

51. M. R. Henn, C. L. Boutwell, P. Charlebois, N. J. Lennon, K. A. Power *et al.*, Whole genome deep sequencing of HIV-1 reveals the impact of early minor variants upon immune recognition during acute infection. *PLoS Pathog* **8**, e1002529 (2012).

52. X. Yang, P. Charlebois, S. Gnerre, M. G. Coole, N. J. Lennon *et al.*, De novo assembly of highly diverse viral populations. *BMC genomics* **13**, 475 (2012).

53. W. Song, D. He, I. Brill, R. Malhotra, J. Mulenga *et al.*, Disparate associations of HLA class I markers with HIV-1 acquisition and control of viremia in an African population. *PLoS One* **6**, e23469 (2011).

54. C. L. Boutwell, J. M. Carlson, T. H. Lin, A. Seese, K. A. Power *et al.*, Frequent and variable cytotoxic-T-lymphocyte escape-associated fitness costs in the human immunodeficiency virus type 1 subtype B Gag proteins. *J Virol* **87**, 3952-3965 (2013).

55. B. N. Kelly, B. R. Howard, H. Wang, H. Robinson, W. I. Sundquist *et al.*, Implications for viral capsid assembly from crystal structures of HIV-1 Gag(1-278) and CA(N)(133-278). *Biochemistry* **45**, 11257-11266 (2006).

56. O. Pornillos, B. K. Ganser-Pornillos, B. N. Kelly, Y. Hua, F. G. Whitby *et al.*, X-ray structures of the hexameric building block of the HIV capsid. *Cell* **137**, 1282-1292 (2009).

57. A. H. Robbins, R. M. Coman, E. Bracho-Sanchez, M. A. Fernandez, C. T. Gilliland *et al.*, Structure of the unbound form of HIV-1 subtype A protease: comparison with unbound forms of proteases from other HIV subtypes. *Acta crystallographica. Section D, Biological crystallography* **66**, 233-242 (2010).

58. Y. Hsiou, J. Ding, K. Das, A. D. Clark, Jr., S. H. Hughes *et al.*, Structure of unliganded HIV-1 reverse transcriptase at 2.7 A resolution: implications of conformational changes for polymerization and inhibition mechanisms. *Structure* **4**, 853-860 (1996).

59. Y. Goldgur, F. Dyda, A. B. Hickman, T. M. Jenkins, R. Craigie *et al.*, Three new structures of the core domain of HIV-1 integrase: an active site that binds magnesium. *Proc Natl Acad Sci U S A* **95**, 9150-9154 (1998).

60. C. H. Lee, K. Saksela, U. A. Mirza, B. T. Chait, J. Kuriyan, Crystal structure of the conserved core of HIV-1 Nef complexed with a Src family SH3 domain. *Cell* **85**, 931-942 (1996).

61. R. Guerois, J. E. Nielsen, L. Serrano, Predicting changes in the stability of proteins and protein complexes: a study of more than 1000 mutations. *Journal of molecular biology* **320**, 369-387 (2002).

62. J. Tang, S. Tang, E. Lobashevsky, A. D. Myracle, U. Fideli *et al.*, Favorable and unfavorable HLA class I alleles and haplotypes in Zambians predominantly infected with clade C human immunodeficiency virus type 1. *J Virol* **76**, 8276-8284 (2002).

63. S. Guindon, J. F. Dufayard, V. Lefort, M. Anisimova, W. Hordijk *et al.*, New algorithms and methods to estimate maximum-likelihood phylogenies: assessing the performance of PhyML 3.0. *Systematic biology* **59**, 307-321 (2010).

64. J. M. Carlson, J. Listgarten, N. Pfeifer, V. Tan, C. Kadie *et al.*, Widespread impact of HLA restriction on immune control and escape pathways of HIV-1. *J Virol* **86**, 5230-5243 (2012).

65. A. Leslie, P. C. Matthews, J. Listgarten, J. M. Carlson, C. Kadie *et al.*, Additive contribution of HLA class I alleles in the immune control of HIV-1 infection. *J Virol* **84**, 9879-9888 (2010).

66. P. C. Matthews, A. Prendergast, A. Leslie, H. Crawford, R. Payne *et al.*, Central role of reverting mutations in HLA associations with human immunodeficiency virus set point. *J Virol* **82**, 8548-8559 (2008).

67. K. H. Huang, D. Goedhals, H. Fryer, C. van Vuuren, A. Katzourakis *et al.*, Prevalence of HIV type-1 drug-associated mutations in pre-therapy patients in the Free State, South Africa. *Antiviral therapy* **14**, 975-984 (2009).

68. P. C. Matthews, E. Adland, J. Listgarten, A. Leslie, N. Mkhwanazi *et al.*, HLA-A*7401-mediated control of HIV viremia is independent of its linkage disequilibrium with HLA-B*5703. *J Immunol* **186**, 5675-5686 (2011).

69. R. L. Shapiro, M. D. Hughes, A. Ogwu, D. Kitch, S. Lockman *et al.*, Antiretroviral regimens in pregnancy and breast-feeding in Botswana. *N Engl J Med* **362**, 2282-2294 (2010).

70. J. Listgarten, Z. Brumme, C. Kadie, G. Xiaojiang, B. Walker *et al.*, Statistical resolution of ambiguous HLA typing data. *PLoS Comput Biol* **4**, e1000016 (2008).

71. J. M. Carlson, C. J. Brumme, E. Martin, J. Listgarten, M. A. Brockman *et al.*, Correlates of protective cellular immunity revealed by analysis of population-level immune escape pathways in HIV-1. *J Virol* **86**, 13202-13216 (2012).

72. D. Bates, M. Maechler, B. Bolker, S. Walker, lme4: Linear mixed-effects models using Eigen and S4. R package. 2013.

73. R Core Team. (R Foundation for Statistical Computing, Vienna, Austria, 2013).

Acknowledgments:

The investigators thank all the volunteers in Zambia who participated in this study and all the staff at the Zambia Emory HIV Research Project in Lusaka who made this study possible. The investigators would like to thank Jon Allen, and Mackenzie Hurlston for technical assistance and sample management, Paul Farmer, Ph.D. for database design and management, and Ilene Brill, Kristin Wall, Xuelin Li, Christoph Lippert, Nicolo Fusi, Jennifer Listgarten, and Zabrina Brumme for helpful discussions. This study was funded by R01 AI64060 and R37 AI51231 (EH) from the National Institutes of Health, and the International AIDS Vaccine Initiative (to SAA), and made possible in part by the generous support of the American people through the United States Agency for International Development (USAID). The contents are the responsibility of the study authors and do not necessarily reflect the views of USAID or the United States Government. This work was also supported, in part, by the Virology Core at the Emory Center for AIDS Research (Grant P30 AI050409); the Yerkes National Primate Research Center base grant (2P51RR000165-51) through the National Center for Research Resources P51RR165 and by the Office of Research Infrastructure Programs/OD P51OD11132; NIH NIAID grants P01-AI074415 (TMA), U01 AI 66454 (RS), T32-AI007387 (RB), and RO1 AI046995 (PG), and the Wellcome Trust (PG). JP, DTC and MS were supported in part by Action Cycling Fellowships. TN was supported by the International AIDS Vaccine Initiative, the South African Department of Science and Technology and the National Research Foundation through the South Africa Research Chairs Initiative, by an International Early Career Scientist award from the Howard Hughes Medical Institute and by the Victor Daitz Foundation. All viral sequences not previously published have been submitted to GenBank—accession numbers JN014076-JN014465, JQ219842, and KM048382-KM050767. The data reported in this paper are tabulated in the Supporting Online Material.

Tables:

Table 1: Donor quasispecies and cohort frequencies as additive predictors of transmission

Feature	γ Estimate[1]	Std. Error	z value	Pr(>|z|)	Likelihood Ratio Test[2] χ^2 (df)	Likelihood Ratio Test[2] Pr(>χ^2)
(Intercept)	7.63	0.557	13.70	<1E-16		
Donor Quasispecies Frequency[3]	0.56	0.053	10.65	<1E-16		
Cohort Frequency (cfreq)[4]	1.98	0.541	3.66	2.5E-4	40.1 (2)	2.0E-9
cfreq^2	0.30	0.121	2.45	0.014		

[1]Fixed effect parameters. Model was fit using logistic regression. Model fit was not improved by the addition of protein domain features or random effects. Compare to Figure 2A in the main text.
[2]Combined significance for sets of features were estimated using the likelihood ratio test.
[3]The standardized smoothed log-odds of the frequency of the amino acid in the donor from deep sequencing. Smoothing factor is $q = 1/50$.
[4]The standardized smoothed log-odds of the frequency of the amino acid in the cohort. Smoothing factor is $q = 1/350$.

Table 2: Multilevel multivariable logistic regression model of transmission selection bias

Feature	γ Estimate[1]	Std. Error	z value	Pr(>|z|)	Likelihood Ratio Test[2] χ^2 (df)	Likelihood Ratio Test[2] Pr(>χ^2)
(Intercept)	6.43	0.558	11.53	<1E-16		
Cohort Frequency (cfreq)[3]	1.70	0.119	14.24	<1E-16		
cfreq^2	0.24	0.019	12.28	<1E-16		
# Covarying sites	0.04	0.012	3.35	8.2E-4		
Susceptible to Recipient HLA	-0.60	0.142	-4.18	2.9E-5		
Donor Esc Polymorphism : Gag[4,5]	0.00	0.253	0.00	0.998		
Donor Esc Polymorphism : Pol	-0.69	0.197	-3.49	4.9E-4	13.3 (3)	0.004
Donor Esc Polymorphism : Nef	0.48	0.326	1.48	0.140		
Risk Index[5]	0.15	0.084	1.74	0.081		
Risk Index : cfreq[6]	0.14	0.067	2.15	0.032	22.2 (3)	5.9E-5
Risk Index : cfreq^2	0.06	0.015	3.65	2.6E-4		
ETI	-0.16	0.132	-1.18	0.236		
p17[7]	0.22	0.228	0.97	0.333		
p17 : cfreq	0.19	0.103	1.83	0.067		
p24	1.72	0.285	6.03	1.7E-9		
p24 : cfreq	0.64	0.116	5.47	4.6E-8		
p15	0.65	0.241	2.71	0.007		
p15 : cfreq	0.28	0.106	2.66	0.008		
Protease	0.62	0.307	2.03	0.042		
Protease : cfreq	0.15	0.135	1.09	0.278		
RT	0.62	0.208	2.98	0.003		
RT : cfreq	0.15	0.095	1.60	0.109		
Integrase	0.50	0.225	2.23	0.026		
Integrase : cfreq	0.19	0.105	1.78	0.076		
Nef	0.97	0.236	4.12	3.8E-5		
Nef : cfreq	0.41	0.310	1.34	0.181		
Nef CD4/MHC Domains	0.50	0.104	4.80	1.6E-6		
Nef CD4/MHC Domains : cfreq	0.52	0.133	3.88	1.0E-4		
Structural Frequency (sfreq)[8]	0.33	0.144	2.29	0.022		
sfreq : cfreq	0.49	0.129	3.80	1.5E-4	24.2 (3)	2.2E-5
sfreq : cfreq^2	0.13	0.029	4.45	8.6E-6		

Random Effects[9]	Std. Dev.	Corr
(Intercept)	0.91	
cfreq	0.08	-1.00

[1]Fixed effect parameters. Model was fit using multilevel logistic regression. Model fit was not improved by the addition of quadratric interaction effects between cohort frequency and protein domains or couple ID. See methods for feature definitions. Compare to Figures 2 and 3 in the main text.
[2]Likelihood ratio test performed between full model and a model excluding the grouped set of features.
[3]Cohort frequency was standardized (zero mean, unit variance).
[4]Donor CTL escape features were scaled by 1−cfreq to reflect the probability that *de novo* escape occurred in the donor.
[5]Colon (:) signifies a multiplicative interaction.
[6]Standardized (zero mean, unit variance) donor VL plus one if the recipient if female or a male with GUI.
[7]Protein domain features are treated as covariates. It is not clear whether significance implies a different relationships between cohort frequency and odds of transmission, or simply reflect variations in mean donor quasispecies diversity.
[8]Defined as the expected frequency of an amino acid in the cohort based on the impact of that amino acid on the protein structure (see methods; frequency was standardized). Structural features were evaluated separately from the rest of the model because crystal structures are available for only a subset of sites. Model estimates reflect model fit using all parameters. Likelihood ratio test is against a null model including only the main parameters, but fit on sites with structural information.

[9]Random effects were applied to each couple. The intercept and the slope of cohort frequency were allowed to vary as a bivariate Guassian. Maximum likelihood standard deviations are reported. The maximum likelihood covariance term is presented as a correlation.

Figures Legends:

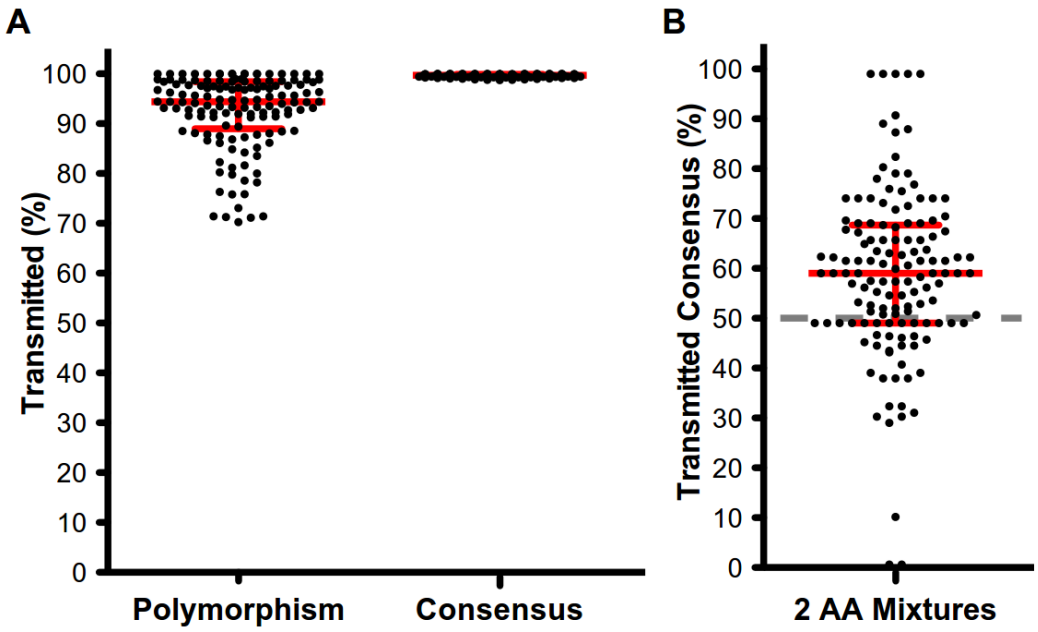

Fig. 1. HIV-1 viruses with amino acid residues matching the consensus of the study population are preferentially transmitted. For each linked transmission couple, the proportion of sites that were transmitted was defined to be the proportion of sites in which the variant observed in the recipient matched that observed in the donor. Sites with a mixture in the recipient were excluded. (**A**) Donor variants that matched cohort consensus were more likely to be transmitted among all non-mixture sites in the donor, while (**B**) a consensus residue that was observed in mixture with one other variant was more likely to be transmitted than was the other variant. A nucleotide mixture was called if more than one base resulted in a >25% Sanger peak height. An amino acid mixture was called if the nucleotide mixture resulted in a mixture of amino acids. Dashed gray line represents the expected frequency of transmission of consensus. Consensus was defined to be any amino acid observed in at least 50% of chronically infected individuals in the Zambian cohort.

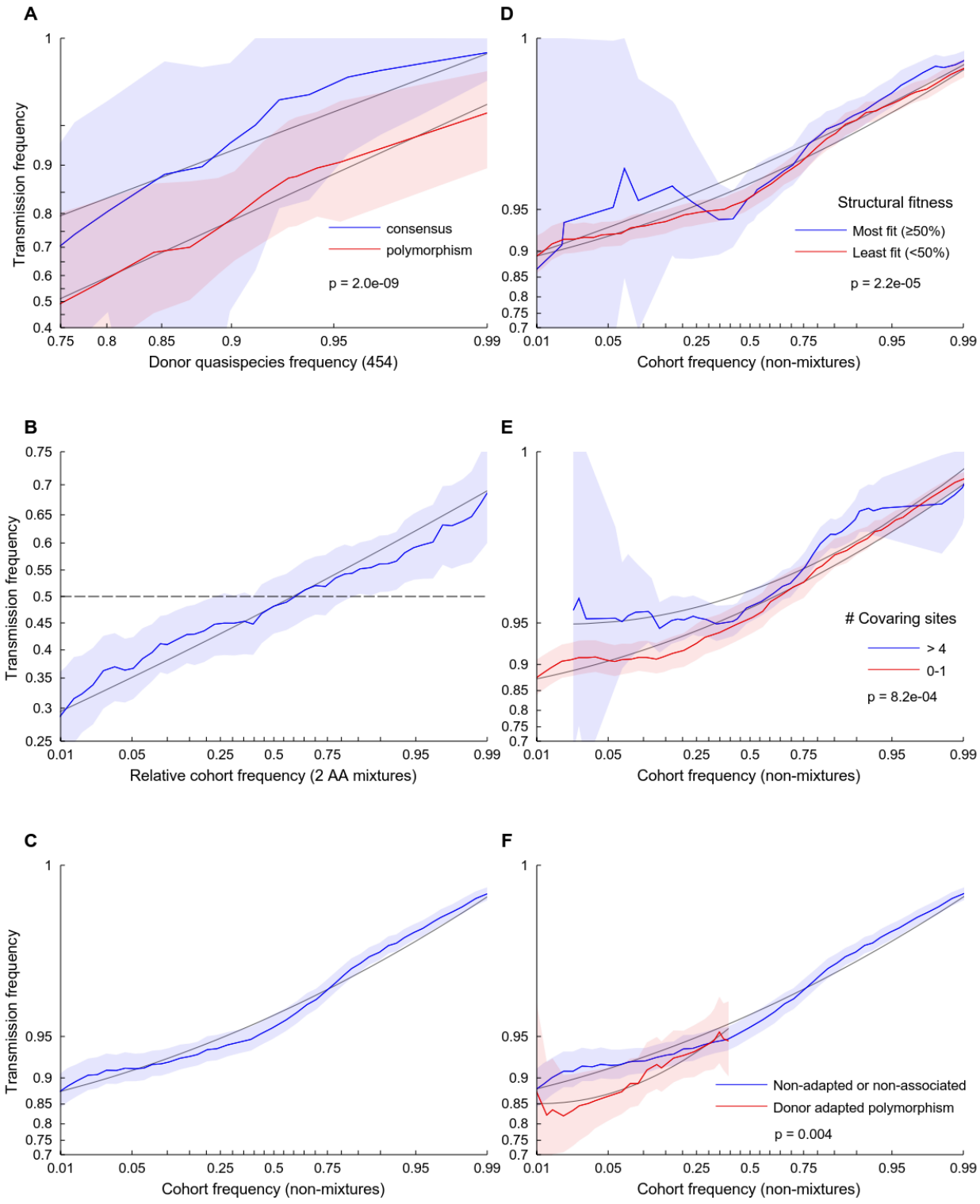

Fig. 2. Viral fitness modulates selection bias in heterosexual HIV-1 transmission. The odds that the donor's amino acid will be transmitted to the recipient is a function of the relative

frequency of the amino acid in the quasispecies as well as the fitness of that amino acid, as estimated here by several independent metrics. Each plot shows the empirical transmission probability (odds on a $\log_{10}$ scale) of a variant as a function of one or more parameters. Empirical transmission probabilities (solid colored lines) are estimated counting the proportion transmitted within a continuous sliding window of width 1 log-odds with respect to the feature represented on the abscissa. All log-odds values are smoothed by adding a pseudo-count. Grey lines represent a quadratic fit to the sliding window averages; shaded areas represent 95% confidence intervals estimated using the percentile-*t* method on 1000 multilevel bootstraps. P-values are taken from Table 1 (A) or Table 2 (D-F) and represent the p-value from a multilevel logistic regression model in which all features are treated as continuous variables, as described in Materials and Methods. (**A**) The log-odds of transmission is linearly related to the relative *in vivo* frequency of the variant in the donor quasispecies, with a near 1-to-1 mapping for variants that match cohort consensus. In contrast, polymorphisms are uniformly less likely to be transmitted (N=8314 observations over 5 couples). (**B**) Among N=3,115 donor sites containing two-amino acid mixtures from 137 couples, the probability of transmission is also strongly predicted by the relative cohort frequency of the amino acid. Transmission probability is with respect to a randomly chosen member of the mixture; the abscissa represents the relative frequency of that amino acid in the cohort compared to the other amino acid in the mixture. (**C-F**) Among N=228,362 non-mixture donor sites from 137 couples, the odds of transmission is predicted by: (**C**) the frequency of the amino acid in the cohort; (**D**) the relative impact of the variant on the stability of the protein structure (low impact implies high fitness); (**E)** the number of covarying sites statistically linked with the variant; and **(F)** whether the variant is consistent with immune escape from one of the donor's HLA alleles (only polymorphic sites are shown). See methods for feature definitions.

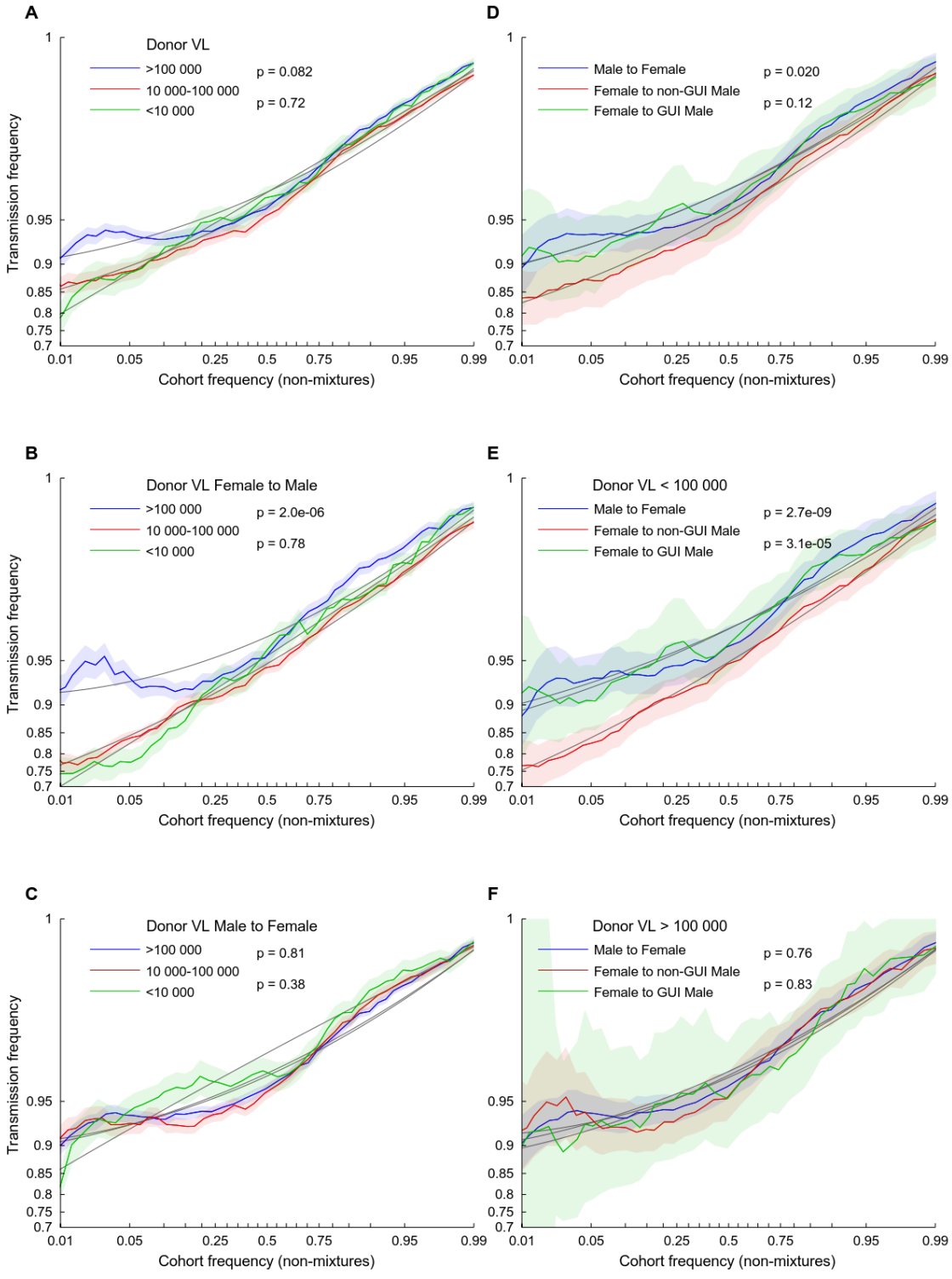

Fig. 3. Transmission risk factors reduce selection bias in heterosexual HIV-1 transmission.

The empirical log-odds of transmission is plotted as a function of the frequency of each variant

in the cohort, as defined in Figure 2. Donor viral load (VL) near the time of transmission, sex of the recipient, and presentation of genital ulcers or inflammation (GUI) in male recipient partners each affect the selection bias. **(A-C)** Individuals are segregated by donor VL levels used in previous studies of transmission risk (*27, 28*). High donor VL reduces transmission selection bias in **(B)** female-to-male, but not **(C)** male-to-female, transmission. **(D-F)** Male recipients appear to have increased selection bias compared to female recipients, an effect that is mitigated by the presence of GUI **(D, E)** or high donor VL **(F)**. 95% confidence intervals (shaded area) and quadratic polynomial fit (solid gray lines) were estimated as in Figure 2. P-values are estimated from a non-parametric, block-bootstrap method that tests the null hypothesis that the normalized area under two curves are identical (see methods for details).

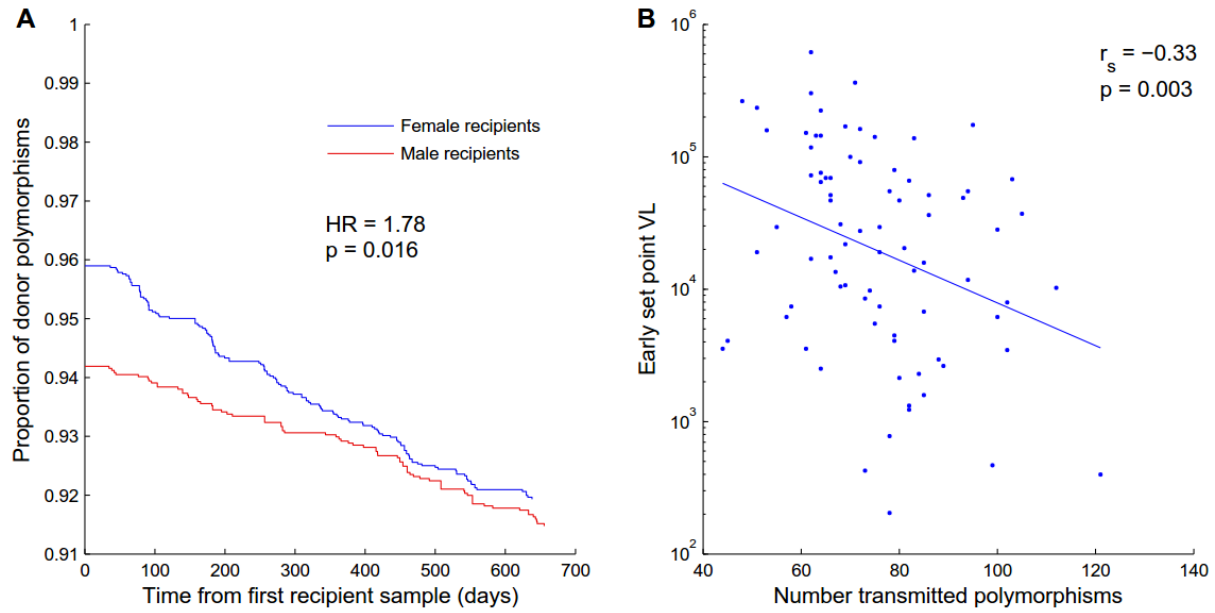

Fig. 4. Transmission of low-fitness viruses changes reversion dynamics and predicts lower early set-point viral load in the recipient. (A) The proportion of donor non-consensus, polymorphisms that remain polymorphic, is plotted as a function of days after the first available recipient sample (N=6,220 polymorphisms from 81 couples). The ordinate at time 0 represents the fraction of donor polymorphisms that were transmitted. Female recipients permit transmission of more polymorphisms than males, but these revert at a faster rate. Hazard ratio and p-value was taken from a multivariable Cox-proportional hazard model (see Table S2). See Figure S4 for estimates of instantaneous reversion rates as a function of time since the estimated date of infection. (B) The number of transmitted polymorphisms at sites that were polymorphic in the linked donor negatively correlates with early set-point VL in the recipient (N=81), corroborating the fitness cost imposed by many of these variants.

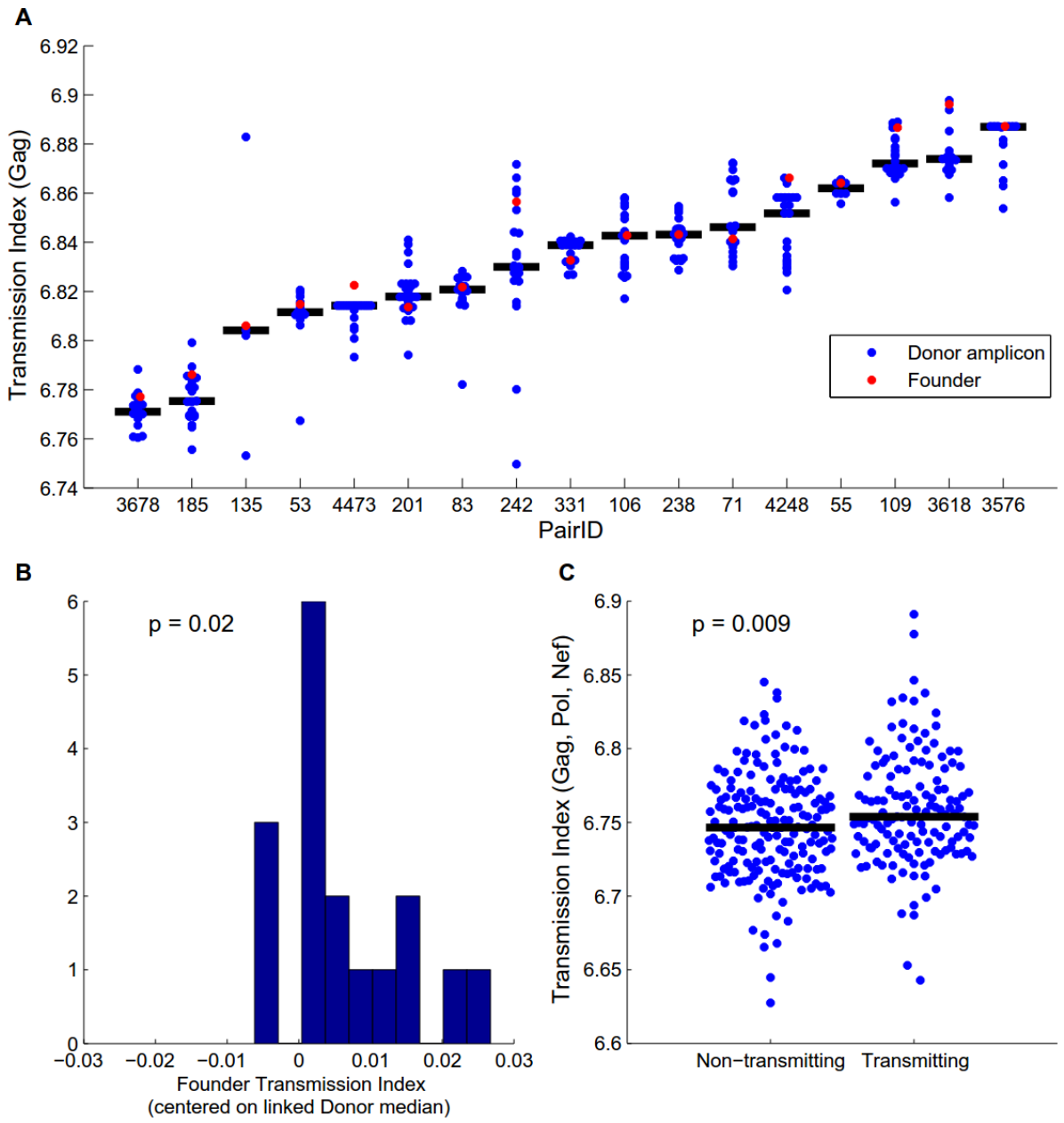

Fig. 5. Sequence-derived transmission index predicts transmission. The transmission index of a sequence was calculated as the mean of the expected log-odds of transmission for each site in the sequence, as estimated by logistic regression model that included a second-order polynomial of cohort frequency, the number of covarying sites, and offsets and cohort frequency interactions for each protein domain. Transmission indices were computed out-of-sample using leave-one-out cross validation. (**A-B**) The transmission index for individual donor Gag amplicons compared to the transmission index for the linked founder Gag sequence. Models

trained on Gag alone. (**A**) Transmission index for each couple. Black bar represents median transmission index of donor sequences. Four sequences with transmission index < 6.7 were excluded as outliers. (**B**) The transmission index of each founder virus, median-centered against the transmission indices for linked donor sequences (*p*-value from two-tailed Wilcoxon signed-rank test). (**C**) The overall transmission index of Gag, Pol and Nef is significantly different between donor and potential source partners in risk-matched discordant couples (*p*-value from two-tailed Mann-Whitney rank-sum test).

Methods

Study subjects

All participants in the Zambia Emory HIV Research Project (ZEHRP) discordant couples cohort in Lusaka, Zambia were enrolled in human subjects protocols approved by both the University of Zambia Research Ethics Committee and the Emory University Institutional Review Board. Prior to enrollment, individuals received counseling and signed a written informed consent form agreeing to participate. The subjects selected from the cohort were initially HIV-1 serodiscordant partners in cohabiting heterosexual couples with subsequent intracouple (epidemiologically linked) HIV-1 transmission (*46-48*). Epidemiological linkage was defined by phylogenetic analyses of HIV-1 *gp41* sequences from both partners (*49*). Viral isolates from each partner in the transmission pair were closely related, with median and maximum nucleotide substitution rates of 1.5 and 4.0%, respectively. In contrast, median nucleotide substitution rate for unlinked HIV-1 C viruses from the Zambian cohort and elsewhere was 8.8% (*49*). The algorithm used to determine the *estimated date of infection* (EDI) was previously described by Haaland *et al.* (*3*). All patients in this cohort were antiretroviral therapy naïve. Zambian linked recipients were identified with a median [IQR] estimated time since infection (ETI) of 46 [42-60.5] days, at which time plasma samples were obtained from both the *transmitting source partner* (donor) and the *linked seroconverting partner* (recipient). All of the transmission pairs included in this study are infected with subtype C HIV-1.

A control group of 181 *Not Yet Transmitting* (NYT) HIV positive partners were selected from discordant couples enrolled for a minimum of 1 year, and matched as a group with the transmitting couples for a risk factor score derived from data on recent 1) sexual activity with the primary partner, 2) sperm count in vaginal wash of female partner, 3) pregnancy history and 4) genital ulcer or inflammatory (GUI) disease. These factors were used to create a risk profile for every transmission pair, and then NYT partners in each of four successive risk strata were selected in the same proportion to the representation of donor in each of the four strata, so that the two sets of HIV positive partners were frequency matched by their risk profile.

Summary statistics for donor and NYT individuals are available in Table S1.

Parameter definitions and methods

Amplification and sequencing of *gag, pol,* and *nef* genes

Viral RNA was extracted from 140 µL of plasma samples using the Qiagen viral RNA extraction kit (Qiagen) and eluted in 60 µl of elution buffer. *Gag-pol* population sequences were generated using nested gene specific primers. Combined RT-PCR and first round synthesis was performed using SuperScript III Platinum One Step RT-PCR (Invitrogen) and 5 µL viral RNA template. RT-PCR and first round primers include GOF (forward) 5' ATTTGACTAGCGGAGGCTAGAA 3' and VifOR (RT-PCR and reverse) 5' TTCTACGGAGACTCCATGACCC 3'. Second round PCR was performed using Expand High Fidelity Enzyme (Roche) and 1 µL of the first round PCR product. Nested second round primers include GIF (forward) 5' TTTGACTAGCGGAGGCTAGAAGGA 3' and VifIR (reverse) 5' TCCTCTAATGGGATGTGTACTTCTGAAC 3'. *Nef* sequences were generated in a similar fashion, using an additional set of nested gene specific primers. RT-PCR and first round primers include Vif1 (forward) 5' GGGTTTATTACAGGGACAGCAGAG 3' and OMF19 (RT-PCR and reverse) 5' GCACTCAAGGCAAGCTTTATTGAGGCTTA 3'. Second round primers include Vif2 (forward) 5' GCAAAACTACTCTGGAAAGGTGAAGGG 3' and OMF19 (reverse). An average of 800 RNA templates were added to the One Step RT-PCR reaction. Three positive amplicons per individual were pooled, representing on average 2400 input genomes, and purified via the Qiagen PCR purification kit (Qiagen). Purified products were sequenced by the University of Alabama at Birmingham DNA Sequencing Core. Sequence chromatograms were analyzed using Sequencher 5.0 (Gene Codes Corp.) and degenerate bases were denoted using the International Union of Pure and Applied Chemistry (IUPAC) codes when minor peaks exceeded 25% of the total peak height in both forward and reverse reads. Codons containing degenerate bases were defined as *mixtures*, whereas those with no evidence of degenerate bases or with minor peaks comprising less than 25% of the total were defined as *dominant variants.*

Sequences were codon aligned to the HXB2 reference sequence using HIVAlign (http://www.hiv.lanl.gov/content/sequence/VIRALIGN/viralign.html), followed by hand-editing. For all analyses, we considered sites where a dominant variant was identified and we excluded sites where a gap or a stop codon was present. In cases where transmission was considered, a site

was excluded if a mixture, gap or stop codon was observed in either the donor or the recipient. For transmission indices, exclusion criteria were based on the sequence in question alone—no information was taken from the individual's partner. For a given couple, a residue was defined to have been *transmitted* if the same amino acid was observed in both donor and recipient. For Figure 2B (transmission from mixtures), we limited the analysis to mixtures consisting of two amino acids in the donor, then randomly selected one of the residues to test if it transmitted. For Figure 1B (proportion of mixtures that transmitted consensus), we limited the analysis to donor mixtures consisting of two amino acids, one of which matched cohort consensus, then measured the per-couple proportion of these sites in which the consensus residue was transmitted.

Protein domains were used as covariates in the modeling. Protein domains were defined as follows: Gag was split into p17, p24 and p15; Pol was split into Protease (Pr), Reverse Transcriptase (RT), Integrase and the Gag-Pol transframe (GagPolTF) region. The CD4- and MHC- downregulation domains of Nef, here defined as HXB2 positions 2, 17–26, 57–58, 62–65, 69–81, 154–155, 164–165, and 174–175 (*50*), were treated as a separate Nef domain.

454 sequencing was performed on five donors to estimate the quasispecies frequency of donor variants. For each donor, we amplified from an average of 13,000 RNA templates and obtained two overlapping PCR amplicons spanning the entire protein-coding region of the HIV-1 genome. Pooled amplicons were acoustically sheared to produce fragments between 300-800 bases in length. Batched, bar-coded samples were amplified by emulsion PCR and sequenced on a 454 Junior (Roche) as described previously (*51*). To achieve sufficient detection of minor variants we required a targeted coverage per site of 250 fold. The raw sequence output ("reads") were assembled by *Vicuna* (*52*) and *V-FAT* (Broad Institute, http://www.broadinstitute.org/scientific-community/science/projects/viral-genomics/v-fat) to form a single genome which represents the majority base at each nucleotide position (the consensus assembly). The reads were then corrected for systematic 454 errors such as homopolymer indels and carry forward/incomplete extensions (CAFIE) and aligned to the consensus assembly using previously developed software RC454 and *V-Phaser* (*51*) as well as with custom programs written in Perl. These alignments were hand-refined to match the corresponding population sequences. Codon positions in which the 454-derived dominant variant differed from the Sanger sequencing-derived amino acid were

excluded. The quasispecies frequency of a codon was taken to be the fraction of reads spanning a codon position that contained the codon. Amino acid frequencies were defined to be the sum of the frequencies of codons encoding the same amino acid. Sites with a read-depth of less than 10 were excluded.

Limiting dilution, single genome amplification (SGA) sequencing of *gag* was performed on 11 donor-recipient pairs, as previously described (*3*) but using *gag*-specific primers. Briefly, full-length *gag* was amplified from PBMC DNA by nested PCR using primers: outerfor1 5' AAGTAAGACCAGAGGAGATC-TCTCGAC 3', gagR2b 5' GCCAAAGAGTGATTTGAGGG 3', innerfor1 5' TTTGACTAGCGGAGGCTAGAAGGA 3' and innerrev1 5' GTATCATCTGCTCCTGTGTCTAAGAGAGC 3'. In addition, 6 pairs of *gag* SGA sequences were extracted from near-full length genome sequences amplified by similar methods to those described previously (*44*). Sequences were aligned to the cohort Sanger sequence alignments.

Cohort frequencies were defined with respect to sequences taken from 375 (*gag*), 327 (*pol*), or 350 (*nef*) chronically-infected individuals in the Zambian cohort. The donor and NYT individuals studied here were the subset for whom *gag*, *pol* and *nef* sequences were available. The cohort frequency was taken to be the proportion of individuals with a given amino acid, excluding all individuals with gaps, stop codons or missing data at the site in question. Amino acid mixtures containing k amino acids contributed $1/k$ observations to each amino acid in the mixture. *Cohort consensus* was defined to be residues observed in a majority (≥50%) of sequences, while *polymorphism* was defined as all non-majority (<50%) residues. All residues at highly polymorphic sites in which no residue was observed in at least half the population were thus defined as polymorphisms.

Smoothed log-odds ratios were used to transform cohort and quasispecies frequencies as input variables for the logistic regression models, as well as for visualization of cohort, *in vivo* and transmission frequencies. The smoothed log-odds account for finite sampling by including a prior that pushes log-odds ratios toward 0. For a probability p with smoothing factor $q, q \in [0,1]$, the smoothed log odds ratio is defined as $slod(p) = \log(p + q) - \log(1 - p + q)$, which is equivalent to adding a pseudo-count of qN if the probability is a proportion derived from N

observations. Here, we use $q = 1/350$ for cohort frequencies and $q = 1/50$ for quasispecies frequencies. For visualization, empirical transmission frequencies are smoothed by the same factor as the variable to which it is being compared.

Virologic and clinical parameters

HIV *plasma viral load* (VL) was determined at the Emory Center for AIDS Research Virology Core Laboratory using the Amplicor HIV-1 Monitor Test (version 1.54; Roche). *Early set point* VL in recipients was defined as the earliest stable nadir VL value measured between 3 and 9 months post infection and which did not show a significant increase in value within a 3-4 month window., as previously described (*19*). Donor VL was defined as the VL determined at or near the time of seroconversion in the previously HIV negative partner.

Genital Ulcers or Inflammation (GUI) in the linked recipient was defined as at least one instance where genital inflammation or ulceration was noted on a physical or was treated between enrollment and seroconversion or during the 12 month period prior to seroconversion for individuals enrolled for greater than 12 months, as previously described (*53*). Recipient GUI data were missing for three men and three women.

Physics-based estimation of structural impact of point mutations

One possible mechanism by which a mutation can reduce overall fitness is by altering the stability of the viral protein. We therefore used an *in silico* estimate of protein stability to estimate the impact of a point mutation on the viral structure, then used these estimates to define the *energy-based expected frequency* of each amino acid. In particular, we first estimated the thermodynamic stability changes caused by each of the 20 amino acids at each site using the FoldX software package (http://foldx.crg.es), as previously described (*54*). Briefly, the structures of p17 (Protein Data Bank [PDB] code: 2GOL) (*55*), p24 hexamer (PDB:3H4E) (*56*), Protease dimer (PDB:3IXO) (*57*), RT (PDB:1DLO) (*58*), Integrase (PDB:1BIS) (*59*), and Nef (PDB:1EFN) (*60*), were mutated to the clade C consensus sequence (as defined by the consensus of our combined southern African cohort) and the FoldX optimization procedure and probability-based rotamer libraries were used to remove steric clashes and other estimation errors and to reconstruct missing side chain atoms (*61*). Then the absolute changes $|\Delta\Delta G|$ in the Gibbs free

energy were estimated using the FoldX software for each of the 20 amino acids. Next, we converted these predicted changes in free energy into a probability distribution for each site. The structurally-based expected frequency $E_s[f_{ij}]$ (*structural frequency*) of amino acid j and site i was defined using a normalized negative exponential (Boltzmann distribution)

$$E_s[f_{ij}] = \frac{\exp(-|\Delta\Delta G_{ij}|)}{\sum_{k=1}^{20} \exp(-|\Delta\Delta G_{ik}|)}.$$

This measure thus captures the relative impact on the structure of the 20 amino acids at a given site: if all amino acids results in roughly the same protein stability, then the expected frequency of each amino acid will be 1/20. We use the absolute value of the change in Gibbs free energy on the assumption that the structural stability of the viral protein is optimized *in vivo*. Thus, by construction, all consensus residues will have $|\Delta\Delta G_{ij}| = 0$. Nevertheless, the expected frequency of consensus residues at different sites will vary, based on the predicted impact of the other residues at each site.

The smoothed log-odds of $E_s[f_{ij}]$, with smoothing factor $q = 1/350$ to match cohort frequency smoothing, was then used as a feature in the models. Estimated values for structural frequency ($E_s[f_{ij}]$) are available in Table S4.

HLA-HIV associations and covariation

For HLA-class I genotyping, genomic DNA was extracted from whole blood or buffy coats (QIAamp blood kit; Qiagen). HLA class I genotyping relied on a combination of PCR-based techniques, involving sequence-specific primers (Invitrogen) and sequence-specific oligonucleotide probes (Innogenetics), as described previously (*62*). Ambiguities were resolved by direct sequencing of three exons in each gene, using kits (Abbott Molecular, Inc.) designed for capillary electrophoresis and the ABI 3130*xl* DNA Analyzer (Applied Biosystems).

Correlations between HIV amino acids and HLA types were estimated using a phylogenetic dependence network, as previously described (*24*). Briefly, a maximum-likelihood phylogeny was estimated for each protein using Phyml (version 3.0; (*63*)), using the general time reversible

substitution model, a gamma distribution over substitution rates, and inferred nucleotide and constant site probabilities. A phylogenetically-corrected logistic regression model (*64*), conditioned on the PhyML-inferred phylogenies, was then used to assess the significance of an HLA allele in determining the amino acid for a given site. Forward selection was used to identify HLA alleles that correlate with a given amino acid at a given site. The model was run twice: once including other sites as covariates (covariation), and once without. To increase power, all variables were treated as binary, and all residues were tested against all HLAs (at "4-digit" subtype and "2-digit" type levels). All associations significant at $q<0.2$ (corresponding to a false discovery rate of 20%) in either run are available in Table S4.

An amino acid at a given site in a given individual was defined to be *consistent with escape* in that individual if: (1) the individual expresses an HLA with an association at that site; and (2) either the residue is positively correlated (referred to as *Adapted* in the literature) with the HLA, or any other residue is negatively correlated (referred to as *NonAdapted* in the literature) with the HLA. *Donor escape* is thus a binary variable that indicates whether the residue is consistent with escape from the donor. In multivariable models, we weight the donor escape binary variable by the probability that escape was selected in the donor, which is estimated one minus the frequency of the residue in the cohort. A residue is *susceptible* to an individual if (1) the individual expresses an HLA with an association at that site; and (2) the residue is negatively correlated (*NonAdapted*) with that HLA. Recipient *Susceptible* is thus a binary variable that indicates whether an amino acid is putatively susceptible to the recipient. We limited analyses to associations identified at $q<0.01$, indicating that 99% of the associations are expected to be non-spurious. These generally represent the strongest associations and are characterized by higher escape frequencies in individuals expressing the HLA and lower background frequencies in individuals not expressing the HLA.

Covariation among HIV sites was determined using the phylogenetically-corrected logistic regression. However, rather than building a dependency network using forward selection, we liberally kept all pairwise associations significant at $q<0.01$. Thus, a mutation at site *a* that initiates a chain reaction of compensation at sites *b* followed by *c*, will be picked up as two separate covarying sites under the pairwise analysis. Thus, this pairwise analysis, while

identifying indirect associations, will characterize the breadth of downstream compensation events expected to result from a given point mutation. We defined the *number of covarying sites* (*# Covarying sites*) of a particular amino acid at a particular site to be the number of unique positions that were significantly associated (positively or negatively) with that amino acid. The number of covarying sites for each amino acid are available in Table S4.

HLA and covariation associations were trained on a multi-cohort dataset of 2,066 chronically clade C infected, antiretroviral-naïve individuals with HIV sequence and high resolution HLA type information. These cohorts have been previously described, but were here merged together for the first time to yield greater statistical power. Briefly, in addition to the Zambian individuals described above (n=360), the cohort consists of individuals from Durban, South Africa (n=968) (*65*, *66*), Bloemfontein, South Africa (n=260) (*67*), Kimberley, South Africa (n=26) (*68*), Gaborone, Botswana (n=386) (*69*), and southern African subjects attending outpatient HIV clinics in the Thames Valley area of the United Kingdom (n=66), originally from Botswana, Malawi, South Africa and Zimbabwe (*68*). From these individuals, population sequences were available for Gag-p17/p24 (n=1897), Gag-p15 (n=1135), Pol-Pr (n=1315), Pol-RT(n=1364), Pol-Int (n=698) and Nef (n=1336). High-resolution HLA types were missing or ambiguous for at least one allele in 239/2066 (11.5%) of non-Zambian individuals. For these, a probability distribution over haplotypes was estimated using a machine learning approach that infers haplotype frequencies, as previously described (*70*) and extensively validated for this purpose (*71*). The inferred HLA completion probability distributions were used as a prior for the phylogenetic-logistic regression analysis, as previously described (*71*).

Statistical modeling of transmission selection bias

Infection as a binomial process

The observation that the majority (>99%) of sexual encounters among heterosexual partners do not result in transmission, coupled with the observation that the majority of transmissions are established by a single founder virus, implies that this process is stochastic. Here, we assume that the number of transmitted founder viruses is distributed binomially, parameterized by the number of viruses in the donor genital compartment and the probability that each virus will

establish infection. We then build on this model to estimate the probability that the founder virus population contains a particular genotype, and use this to model selection bias.

Suppose the average sexual encounter is characterized by n viruses present in the infected partner's genital compartment, and that *a priori* probability that any particular virus will establish infection is p. If the probability that a given virus establishes productive infection is independent of the state of other viruses, then the total number T of viruses establishing infection is a binomially-distributed random variable. Of particular interest is the probability that at least one virus establishes infection, providing the rate r of transmission, given by

$$r \stackrel{\text{def}}{=} \Pr(T > 0; n, p) = 1 - (1 - p)^n \approx np, \qquad (2)$$

where the approximation follows from a Taylor series expansion because the rate is small: observed rates of transmission have been reported in the range 0.01–0.001 (*9*).

A model for selection bias

The question of selection bias can now be phrased as the question of whether p depends upon the type of viruses. Suppose the population of viruses in the infected donors is grouped into two types: type a and type $\overline{a}$. Such binarization can be defined arbitrarily, but in this study, we categorize the viruses based on whether they contain the dominant amino acid variant at a particular site (a) or not ($\overline{a}$). Extending the above formulation, we can write $n = n_a + n_{\overline{a}}$ and $p = f_a p_a + (1 - f_a) p_{\overline{a}}$, where $n_a = f_a n$ is the number of viruses of type a, written in terms of the frequency f_a of a in the quasispecies, $n_{\overline{a}} = (1 - f_a) n$ is the number of viruses of type $\overline{a}$, and $p_a, p_{\overline{a}}$ are the *a priori* probabilities that a virus of type a or $\overline{a}$ will establish infection, respectively. Then the total number of transmitted viruses becomes $T = T_a + T_{\overline{a}}$, for binomially-distributed random variables T_a and $T_{\overline{a}}$ that represent the total number of transmitted virons of type a and $\overline{a}$, respectively.

In the context of transmission selection bias, a natural quantity of interest is the odds that a virus of type a is in the population of viruses that establish infection, conditional on infection being established, which is approximately

$$\frac{\Pr(T_a > 0 | T > 0)}{\Pr(T_a = 0 | T > 0)} \approx \frac{\Pr(T_a > 0 | T > 0)}{\Pr(T_{\overline{a}} > 0 | T > 0)} \approx \frac{n_a p_a}{n_{\overline{a}} p_{\overline{a}}} = \frac{f_a p_a}{(1 - f_a) p_{\overline{a}}}, \quad (3)$$

where the first step follows because a and $\overline{a}$ are mutually exclusive and complete and our assumptions of independence and low rates of infection imply that the probability of transmitting both a and $\overline{a}$ is negligible (see Supplementary Note S2). The log of Eq. 3 fits nicely into the logistic regression framework:

$$\ln\left(\frac{\Pr(T_a > 0 | T > 0)}{\Pr(T_a = 0 | T > 0)}\right) = \ln\left(\frac{f_a}{1 - f_a}\right) + \ln\left(\frac{p_a}{p_{\overline{a}}}\right) \quad (4)$$

$$\equiv \beta_f + x\beta, \quad (5)$$

where the offset term β_f estimates $\ln(f_a/(1 - f_a))$, $x = (x_1, \ldots, x_L)$ is a row vector of features and $\beta = (\beta_1, \cdots, \beta_L)$ is a column vector of weights. From Eq. 4 we see that the ratio $p_a/p_{\overline{a}}$ has the effect of biasing the probability that a is in the founder virus, which is otherwise determined by the frequency of a in the donor quasispecies. Thus, we define the *bias with respect to a* to be

$$\text{bias}_a = \ln\left(\frac{p_a}{p_{\overline{a}}}\right) \quad (6)$$

and say transmission is *unbiased* if $\text{bias}_a = 0$. By fitting (β_f, β) to the observed data consisting of all dominant variants observed in all individuals, we can estimate the effects of our L features on selection bias and test the null hypothesis that a given feature has no effect on selection bias (i.e., $\beta_l = 0$).

A key observation of this formulation is that the log-odds that the majority variant is transmitted is equal to the log-odds of the frequency of that variant in the quasispecies, plus or minus some bias term. This is validated in Figure 2A of the main text, where the log-odds transmission probability is equal (within the limits of estimation) to the log-odds quasispecies frequencies for consensus residues, but is shifted down for polymorphisms. This formulation further predicts that donor quasispecies frequency will be the primary determinant of transmission except in the most extreme cases of selection bias, consistent with previous reports (*7*).

The effect of transmission risk factors on selection bias

Transmission risk factors may increase the risk of transmission in one of two ways: (1) by increasing the number of viruses n that have an opportunity to establish infection, for example by increasing VL or increasing the number of sexual exposures; or (2) by increasing the probability p that any one virus can establish infection, either by increasing the transmission fitness of all virus particles, or increasing the susceptibility of the uninfected partner.

A key observation from Eq. 4 is that n is completely absent, indicating that the number of exposures or quantity of virus present at the time of exposure will not alter the selection bias. In contrast, suppose all individual viruses are equally more likely to establish infection (*e.g.*, due to increased susceptibility in the uninfected partner), by a quantity c. Then the selection bias with respect to a becomes

$$\text{bias}_a = \ln\left(\frac{p_a + c}{p_{\bar{a}} + c}\right), \tag{7}$$

which converges toward 0 as c becomes relatively large. Thus, individuals with high risk factors will experience a reduced selection bias, as observed in Figure 3 of the main text. Our observation that VL reduces selection bias in female-to-male transmission indicates that VL increases transmission risk in this population at least in part by serving as a marker of increased transmission fitness, and not simply due to exposure by a higher quantity of virus particles.

The absence of n and the simple form of Eq. 6 are the result of our assumptions of independence of transmission among virions and of a low overall rate of transmission. These assumptions warrant further exploration and are discussed in supplementary notes below.

Multilevel logistic regression (generalized linear mixed models)

Parameter estimation and hypothesis testing under logistic regression assumes independence of observations: in this case, each site in each individual is treated independently. However, as observed in Figure S2, the relationship between cohort frequency and transmission probability differs among proteins (indicating non-independence among sites within the same protein); and as suggested by Eq. 6, all sites within a couple may experience higher or lower transmission probabilities as a result of couple-specific risk factors (indicating non-independence among sites

within the same couple). In this section, we describe our specification of a multilevel, multivariable logistic regression model (also known as a generalized linear mixed model) to account for these non-independences (*26*). A multilevel logistic regression is similar to a standard logistic regression, but with random variables embedded in the definition of some of the coefficients. In the current context, an instantiation of a random variable is indexed by transmission couple, allowing the coefficients to be constant among observations drawn from the same individual, but to vary randomly between individuals.

For N total observations over J proteins in M couples, let p_{ijk} be the probability that the dominant variant observed at position i ($i = 1, \dots, N$) in protein j ($j = 1, \dots, J$) in couple k ($k = 1, \dots, M$) is transmitted. Let $X = \{x_{il}\}$ be a $N \times L$ data matrix of L features. The features of the model are in Table 2 and described in detail in the section entitled "Parameter definitions and methods". Here, we call attention to two features of particular interest: let the column vectors X_c and X_r be the cohort frequencies and risk indices (the aggregate of sex, VL and GUI, defined above) for the observations. Because we call special attention to these features, we define a new $N \times (L-2)$ predictor matrix W, such that $X = [W\ X_c\ X_r]$. Then the multilevel logistic regression is defined by level one:

$$\text{logodds}(p_{ijk}|X) = \beta_{ijk}^{(0)} + \beta_{ijk}^{(1)} x_{ic} + \beta_i^{(2)} x_{ic}^2. \quad (7)$$

This model assumes a quadratic effect between cohort frequency and odds of transmission. (The quadratic polynomial was chosen by first testing a model that included only protein effects and cohort frequency as a cubic on cohort frequency, then observing that the linear and quadratic effects, but not the cubic effects, were significant). Each of the β terms are composite, mixed-effect terms, defined by level two:

$$\beta_{ijk}^{(0)} = \gamma_{00} + W_i\Gamma + \gamma_{0r} x_{ir} + \gamma_{0j} + \epsilon_{0k} \quad (8)$$

$$\beta_{ijk}^{(1)} = \gamma_{10} + \gamma_{1r} x_{ir} + \gamma_{1j} + \epsilon_{1k} \quad (9)$$

$$\beta_i^{(2)} = \gamma_{20} + \gamma_{2r} x_{ir} \quad (10)$$

where Γ is a column vector of fixed effects, the γ terms are fixed effects, with separate γ_{0j} and γ_{1j} terms for each protein domain, and the ϵ terms are random effects, which are normally

distributed as

$$\begin{bmatrix}\epsilon_{0k}\\ \epsilon_{1k}\end{bmatrix} \sim N\left(\begin{bmatrix}0\\ 0\end{bmatrix};\ \Sigma_\theta\right), \theta = (\sigma_0, \sigma_1, \sigma_{01}),$$

with an independent sample taken for each couple k. Thus, the offset $\beta_{ijk}^{(0)}$ (Eq. 8) is determined by a grand mean (γ_{00}), a linear combination of all predictors and their coefficients ($X_i\Gamma$), and protein- and couple- specific offsets; the linear term $\beta_{ijk}^{(1)}$ (Eq. 9) is determined by a grand mean (γ_{10}), the risk ($\gamma_{1r}x_{ir}$), and protein- and couple-specific slopes; and the quadratic term $\beta_i^{(2)}$ (Eq. 10) is determined by a grand mean (γ_{20}) and the risk ($\gamma_{2r}x_{ir}$). Proteins are treated as fixed effects. Because the couples in our study represent a random draw from an assumed population, the couple-specific offset and slope terms ($\epsilon_{0k},\ \epsilon_{1k}$) are treated as random effects, with the effect for any given couple drawn from a bivariate normal distribution in which the offset and slope are allowed to be correlated. The final model learns the variance-covariance matrix Σ_θ, which specifies the level of variability in slope and offset among couples, then integrates out ($\epsilon_{0k},\ \epsilon_{1k}$). The multilevel logistic regression was carried out using the glmer routine of the lme4 package (*72*) in R v3.0.2 (*73*). Protein- and couple- specific linear effects significantly improved the fit of the model ($p<10E-8$ by likelihood ratio test); quadratic effects did not improve the fit ($p>0.4$ for both protein and couple-specific terms). The final fit model is shown in Table 2.

Transmission index

Given a set of features $x = x, \ldots, x_L$, and a trained model $(\beta_f, \beta), \beta = \beta_1, \ldots, \beta_L$, we can compute the expected log-odds of transmission for any residue and any site. We define the *transmission index* of a sequence (or <Gag, Pol, Nef> tuple of sequences) to be the mean log-odds of transmission over all sites in the sequence. Sites containing mixtures, stop codons, or gaps are ignored. To avoid overfitting, models for the transmission index were estimated using leave-one-out cross validation, such that the transmission index for each donor was computed using a model inferred from data that did not include that couple. The NYT transmissibility scores were taken from randomly selected models learned from the leave-one-out donor-recipient training runs to ensure that any differences in observed variance were not due to differential model variance. Transmission indices were computed using a subset of features: log-odds cohort frequency, and its square; the number of statistically-linked covarying sites; and corrections for subproteins (p17,p24,p15, GagPolTF, Protease, RT, Integrase and the Nef functional domain, as

described above). SGA sequences were only available for Gag; we therefore used models trained on Gag alone for Figure 5A-B in the main text. For computational efficiency, random effects were not used in model inference for transmission indices.

Statistical analyses

Empirical transmission probability curves

To visualize the probability of transmission as a function of the frequency of a variant in the cohort or donor quasispecies (Figs. 2,3,S2), we used a sliding window approach in which we measure the observed proportion of sites that were transmitted within a given window. For example, for a given donor quasispecies frequency f, the *empirical transmission probability* corresponding to f is the proportion of all variants i such that $|\text{logodds}(f) - \text{logodds}(f_i)| < w$ for some window size w. The reported values are the empirical transmission frequency and the mean cohort frequency, over all observations within the window. We use $w = 1$, and only includes values of f with at least 20 points in the window.

To estimate 95% confidence intervals for an empirical transmission probability curve, we employ a block bootstrap approach using the percentile-t method (*45*). Briefly, for each of $B = 1000$ bootstrap replicates, we sample with replacement the couples, then the sites within each sampled couple. We then estimate the empirical transmission probability for each cohort frequency value observed in the complete dataset. The percentile-t 95% confidence interval is then estimated independently for each cohort frequency value.

In Figure 3 in the main text, we report p-values for comparing two empirical transmission probability curves (e.g., comparing male-to-female versus female-to-male transmission). The statistic we used was the difference in the mean empirical transmission probability calculated over all cohort frequencies with at least 20 observations within the sliding window. Mean empirical transmission probabilities were calculated using the trapezoid method over the cohort and transmission frequencies output by the sliding window method. We then compared the observed difference in means to a normal distribution with mean 0 and standard deviation $\hat{\sigma}$ to test the null hypothesis that the observed difference between the means of the two curves was

zero. $\hat{\sigma}$ was estimated as the standard deviation of the difference in means observed over the $B = 1000$ bootstrap replicates used to construct the confidence intervals.

Reversion analysis

The rates of reversion from polymorphism to consensus, for sites in which a polymorphism was present in both the donor and recipient, were estimated as a function of fitness and susceptibility features. The date of reversion or loss-to-followup was determined relative to the date of the first available recipient sample. Thus, reversion rates are conditional on a polymorphism being present in both the donor sample and the first recipient sample. (Because we tracked reversion to consensus, the polymorphism in the recipient may differ from that in the donor). The date of reversion was defined as the midpoint between the last non-mixture polymorphism and the first non-mixture consensus, minus the date of the first recipient sample. Mixtures were counted as missing data. Hazard ratios (HRs) were estimated using a Cox proportional hazard model. To account for assumed non-independence among sites sampled from the individuals, a multilevel bootstrap was performed (Level 1 = sites, Level 2 = individuals), with 1000 replicates. Reported HR values are those from the full model. P-values are computed from the standard errors of the bootstrap HR values, assuming a standard normal distribution. Only sites with available structures were used in the Cox proportional hazard model (Table S4); all sites were used for Figure 4 in the main text. Statistical modeling was carried out using Matlab ® (MATLAB and Statistics Toolbox Release 2012b, The MathWorks, Inc., Natick, Massachusetts, United States).

Supplementary Materials for

Selection Bias at the HIV-1 Transmission Bottleneck

Jonathan M. Carlson[#], Malinda Schaefer[#], Daniela Monaco, Rebecca Batorsky, Daniel T. Claiborne, Jessica Prince, Martin J. Deymier, Zachary S. Ende, Nichole R. Klatt, Charles E. DeZiel, Tien-Ho Lin, Jian Peng, Aaron Seese, Roger Shapiro, John Frater, Thumbi Ndung'u, Jianming Tang, Paul Goepfert, Jill Gilmour, Matt A. Price, William Kilembe, David Heckerman, Philip J.R. Goulder, Todd M. Allen, Susan Allen and Eric Hunter

[#] Contributed equally to this manuscript

correspondence to:
JMC: carlson@microsoft.com
EH: ehunte4@emory.edu

This PDF file includes:

Notes S1 and S2
Figs. S1 to S4
Tables S1 to S3

Other Supplementary Materials for this manuscript includes the following:

Table S4

Supplementary Text

Note S1: The role of donor VL in transmission risk and selection bias

In Eq. 6 we noted that an overall increase c in the probability that any donor virus will be able to establish infection will lower the odds of transmission. Notably, transmission risk factors that increase risk by simply increasing exposure (reflected by n, the number of viruses in the quasispecies, which could be generalized to account for the number of exposures) were not present in Eq. 6, having canceled out in prior steps. Importantly, this cancelation was possible because of the assumption that the overall rate of transmission is small, leading to the approximation in Eq. 2. But how good is this approximation and what happens when transmission rates are high, violating the assumption that enables this approximation? This question is particularly relevant for donor VL, a well-established transmission risk factor. Although VL is known to increase transmission risk, there are at least two possible mechanisms: (i) high donor VL is a marker of increased viral fitness, consistent with the observations that *in vivo* replicative capacity correlates with VL (*18-21*) and that donor VL predicts early setpoint VL in linked recipients (*32-34*); and (ii) high donor VL simply increases the probability of transmission by increasing overall exposure. Our observation that increased donor VL reduces transmission selection bias suggests that fitness is at least one factor, but only if the approximation in Eq. 2 is valid.

To explore the validity of the approximation in Eq. 2 in the context of selection bias as expressed in Eq. 4, we implemented the formula for the exact rate of transmission under the binomial distribution in Matlab®, given by

$$r \equiv \Pr(T > 0) = 1 - (1 - p_a)^{f_a n}(1 - p_{\overline{a}})^{(1-f_a)n}$$

then plotted the relationship between r and the conditional probability that the founder virus included a virus of type a (fig. S3), given by

$$r_{a|r} \equiv \Pr(T_a > 0 | T > 0) = \frac{1 - (1 - p_a)^{f_a n}}{1 - (1 - p_a)^{f_a n}(1 - p_{\overline{a}})^{(1-f_a)n}} = \frac{r_a}{r}$$

where $r_a = 1 - (1 - p_a)^{f_a n}$ is the rate of transmission of viruses of type a. If transmission is unbiased, then $p = p_a = p_{\overline{a}}$ and we can write

$$r_{a|r} \equiv \Pr(T_a > 0 | T > 0) = \frac{1 - (1 - p)^{f_a n}}{1 - (1 - p)^n} \approx f_a$$

where the approximation again assumes a low rate of transmission. Thus, for small rates of transmission, transmission will be unbiased with respect to a if $r_{a|r} = f_a$; that is, if the probability that the founder virus includes a virus of type a is equal to the proportion of donor viruses that are of type a. For each simulation experiment, we first set the baseline selection bias $b = (p_a + c)/(p_{\overline{a}} + c)$, the frequency f_a of a in the donor quasispecies, and initial values of n and p_a such that r was low (initially 0.001). Setting $c = 0$, and $n = 1000$, we then manipulated r by increasing either n or c, and then plotted the relationship between r and $r_{a|r}$.

From this experimental setup, we observed that, for very high rates of transmission ($r > 0.5$), the odds that a virus of type a is in the founder population increases due to the increased odds of multiple-virus infection (fig. S3). For cases where selection bias favors the minority variant ($p_a < p_{\overline{a}}$; top rows of fig. S3), increasing the rate of infection by increasing c (that is, increasing the ability of each individual virus to establish infection; blue circles) causes selection bias to shrink toward zero, as seen by the convergence of $r_{a|r}$ toward f_a; this convergence is slowest when a represents 99% of the population, which is close to the mean value of f_a over all sites in our deep sequencing data. In contrast, increasing the quantity of donor viruses, n, has no effect on selection bias: until r is sufficiently high to make multiple-virus infection likely, the probability that the founder includes a remains near f_a. Similar results are observed when the selection bias favors the donor majority variant ($p_a > p_{\overline{a}}$; bottom rows of fig. S3), though here the effect of multiple-virus transmission is to induce a U-shape on the selection-bias curve. Notably, in each of these plots, the approximation in Eq. 3 (solid red and blue lines) closely tracks the exact probabilities for cases of single-virus infection, validating our use of this approximation in the models.

Thus, these simulations confirm that the overall donor viral population size n does not affect transmission selection bias in cases of single-virus transmission, while the effect of multiple-virus transmission is to increase the probability that a virus of type a is transmitted, regardless of the selection bias. In Fig. 3, we observed that increased donor VL predicts lower selection bias and that this effect is strongest for polymorphisms, an observation that is inconsistent with high VL simply increasing the rate of multiple-virus transmission. These results thus suggest that high VL is in this context primarily a marker for increased viral transmission fitness. That donor VL is a more important predictor for transmission in male compared to female recipients [(*27*); see also table S3] is consistent with our observation that female recipients generally have a lower selection bias than males and that donor VL has a stronger effect on selection bias among male recipients (Fig. 3). These observations suggest that the increased effect of donor VL on female-to-male transmission may primarily be the result of an increased barrier among male recipients that increases the importance of overall viral fitness (in effect, c is much smaller in males than females). Together with our observation that transmission index predicts transmission (Fig. 5), these models predict that reduction in overall viral fitness (for example, via drug resistance mutations, or as a result of immunological adaptation), will have a larger effect on female-to-male than on male-to-female transmission.

These results also suggest that therapeutic approaches to lowering VL without lowering VL fitness (for example, anti-retroviral therapy [ARV] in the absence of viral escape) will have no effect on transmission selection bias. Indeed, to the extent that ARV failure is caused by mutations that concomitantly weaken the virus, these models predict that high viral loads resulting from virologic failure will be correlated with *increased* selection bias, as in these cases higher VL will be a marker of *decreased* fitness in the absence of drug due to the escape mutations. Similar effects may arise in the case of elite controllers—if elite control is primarily indicative of an effective immune response and not a general inability of the virus to replicate.

Note S2: Independence of viruses

Thus far, we have assumed that the probability that two different viruses will establish infection are independent of each other. However, it has been reported that the distribution of multiple-virus infections exceeds what would be expected under independence (*1*). Indeed, the rate of multiple-virus infections (≈ 10%) exceeds by 10 to 100 fold what would be predicted from the binomial distribution given observed rates of transmission (see next section). But what is the effect of non-independence on our modeling and on our conclusions?

The hypothesis that transmission is non-independent is supported by the relatively high frequency of multiple-virus infections. One possible mechanism for this non-independence would be a process in which the successful transmission of one virus makes it easier for another virus to break through the physical and immunological barriers (for example, if infection of one target cell causes the recruitment of other target cells). This mechanism would imply that the probability that no viruses establish infection remains $(1-p)^n$, and thus the overall probability of infection is still given by $r = \Pr(T > 0; n, p) = 1 - (1-p)^n$, and the observed low rates of transmission, $r < 0.01$, still allow the approximation $r \approx np$. The primary issue of non-independence is that the frequency of multiple-virus transmission will be non-negligible—roughly 10% in heterosexual cohorts. For these 10% of individuals, the odds that a virus of type a is in the founder population is no longer a simple function of f_a and $p_a/p_{\overline{a}}$ (Eq. 3), because the denominator needs to account for the probability that viruses of both type a and $\overline{a}$ are transmitted. In effect, the odds as stated in Eq. 3 will overestimate the true odds. However, while 10% of individuals are infected with multiple viruses, in our model setup, we group all viruses into two types: type a, comprising >75% of all donor viruses, and type $\overline{a}$. In this context, transmission of multiple viruses is irrelevant if they are all of the same type, as will be the case for the vast majority of sites for any particular instance of multiple-virus transmission. Furthermore, by filtering out instances where a mixture is observed in the recipient, we likely exclude many instances in which the founder population includes viruses from both the donor majority and minority variants. Thus, the overall proportion of sites in our modeling setup that includes viruses of both types is likely much less than 10%.

Nevertheless, what is the effect of non-independence on the small number of sites where this is relevant? With respect to viral fitness features (primarily those in Fig. 2), the effect will be to dilute the signal, making it harder to detect a selection bias between viruses of type a and $\overline{a}$. Thus, non-independence does not change our conclusions with respect to the existence of selection bias at the transmission bottleneck in general, nor the observation that these features are related to viral fitness in particular. With respect to the reduction of selection bias by risk factors, the effect will be to uniformly increase the probability that the founder population includes a virus of type a, regardless of whether selection bias favors or restricts a. Indeed, this can be observed among the high rates of transmission observed in fig. S3 (see Note S1), in which increasing n to very high rates of transmission increases the probability that a is in the founder population, regardless of $p_a/p_{\overline{a}}$. Importantly, while the risk factors considered here (sex, GUI and donor VL) likely increase the rate of multiple-virus transmission [as any transmission risk factor will under the binomial distribution, and as previously reported for GUI (*3*)], the observation that this effect is most extreme among variants with low cohort frequency, where $p_a \ll$

$p_{\overline{a}}$ (Fig. 3), argues that this effect is largely driven by a reduction in selection bias, not by very high rates of multiple-virus transmission.

The expected rate of multiple infection under the binomial distribution is approximately the rate of transmission

We asserted in the previous section that the pattern of multiple-virus infection suggests that transmission is non-independent. This observation was first made by Abrahams and colleagues, who argued from the Poisson distribution that the observed distribution of the number of virus genotypes per infection was not consistent with the independence assumption (*1*). Here, we briefly re-derive the Abrahams result using the binomial distribution and show that, under independence, the proportion of founder populations with more than one virus will be approximately the same as the overall rate of infection. Since the observed rate of multiple-virus infection greatly exceeds that predicted by the binomial distribution, we conclude that transmission is characterized by non-independence among individual viruses, such that the transmission of one virus particle increases the probability that other virus particles will be part of the founder population.

Equation 2 provides the exact probability (assuming a binomial process) that at least one virus establishes infection: that is, the probability, or rate r, of infection per exposure incident. Similarly, the binomial distribution provides the exact probability that a single virus establishes infection as

$$\Pr(T = 1; n, p) = np(1-p)^{n-1}$$

Thus, the conditional probability that productive infection was established by a single virus is

$$\Pr(T = 1 | T > 0; n, p) = \frac{np(1-p)^{n-1}}{1-(1-p)^n}$$

From the approximation in Eq. 2, we see that the probability that a successful transmission event involves multiple viruses is approximately

$$\begin{aligned}\Pr(T > 1 | T > 0; n, p) &= 1 - \frac{np(1-p)^{n-1}}{1-(1-p)^n} \\ &\approx 1 - \frac{n\frac{p}{1-p}(1-np)}{np} \\ &= 1 - \frac{1-np}{1-p} \\ &= 1 - \frac{1-r}{1-\frac{r}{n}} \\ &\approx r\end{aligned}$$

where we have again used the assumption of small per-virus transmission probability, p<<1. That is, the proportion of infections established by multiple variants will be

approximately equal to the proportion of sex acts that result in any infection. Note that while the above approximations allow for an intuitive understanding of the relationship between the probability of transmission and the conditional probability of transmitting multiple viruses, exact probabilities are easily computed by statistical software and reveal that the above approximations *overstate* expected transmissions that involve multiple viruses, especially when the probability of transmission exceeds 20% (data not shown).

Note that, for small transmission rates, the precise values of n and p are irrelevant: np is the statistic of interest, as it determines the transmission probability r. Furthermore, note that this result holds under models in which individual viruses have different probabilities of establishing infection (in which case p represents the mean over the entire population of viruses). For example, it is well known that some couples represent high infection risk, while others represent low infection risk (*27, 28*). In these scenarios, the above model can be extended to a probabilistic hierarchical model, with the same result that the expected number of multiple-virus transmissions will be approximately equal to the overall rate of transmission. Briefly, if high risk couples have a rate of transmission of $r_{\uparrow}$ while low risk couples have a rate of transmission of $r_{\downarrow}$, then the overall rate of transmission in the population will be the average rate of transmission, weighted by the proportion of individuals in the high ($f_{\uparrow}$) or low ($1 - f_{\uparrow}$) risk groups. Similarly, because within each group the rate infection will be approximately the same as the rate of infections involving multiple viruses, the conditional probability that productive transmission results in multiple transmitted viruses will also be the weighted average $r \approx f_{\uparrow} r_{\uparrow} + (1 - f_{\uparrow}) r_{\downarrow}$. That is, the overall rate of transmission will still be approximately equal to the overall proportion of transmissions that involve multiple transmitted viruses.

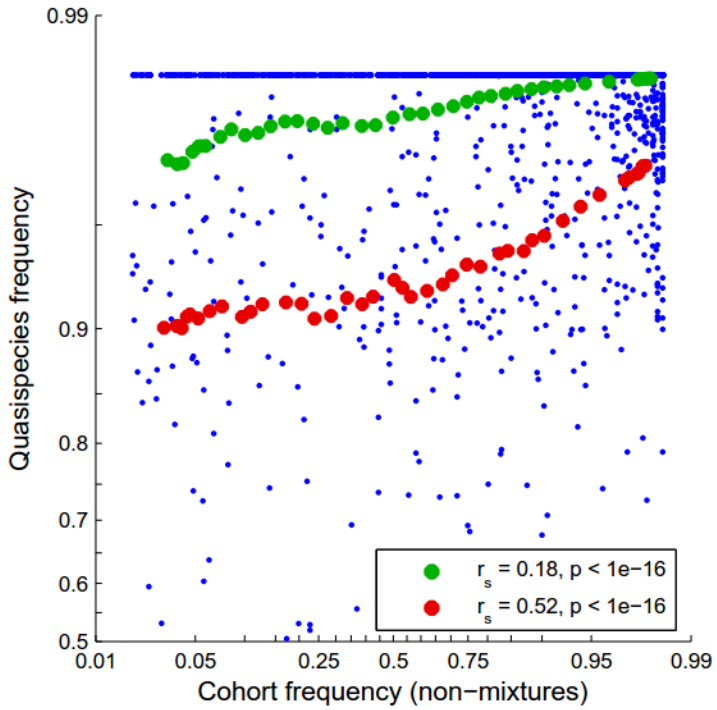

Fig. S1. Cohort frequencies of donor majority variants correlate with the frequency of those variants in the donor quasispecies.

Deep sequencing (454) was performed on 5 donors to estimate the quasispecies frequencies of dominant variants, as called from population sequences. The mean quasispecies frequency computed as a sliding window over cohort frequency (window size of 1 unit in log-odds space) is plotted in Green (all sites) and Red (all sites with observed quasispecies variation in the donor). Cohort and quasispecies frequencies are computed as smoothed log-odds scores with smoothing factor $q = 1/50$.

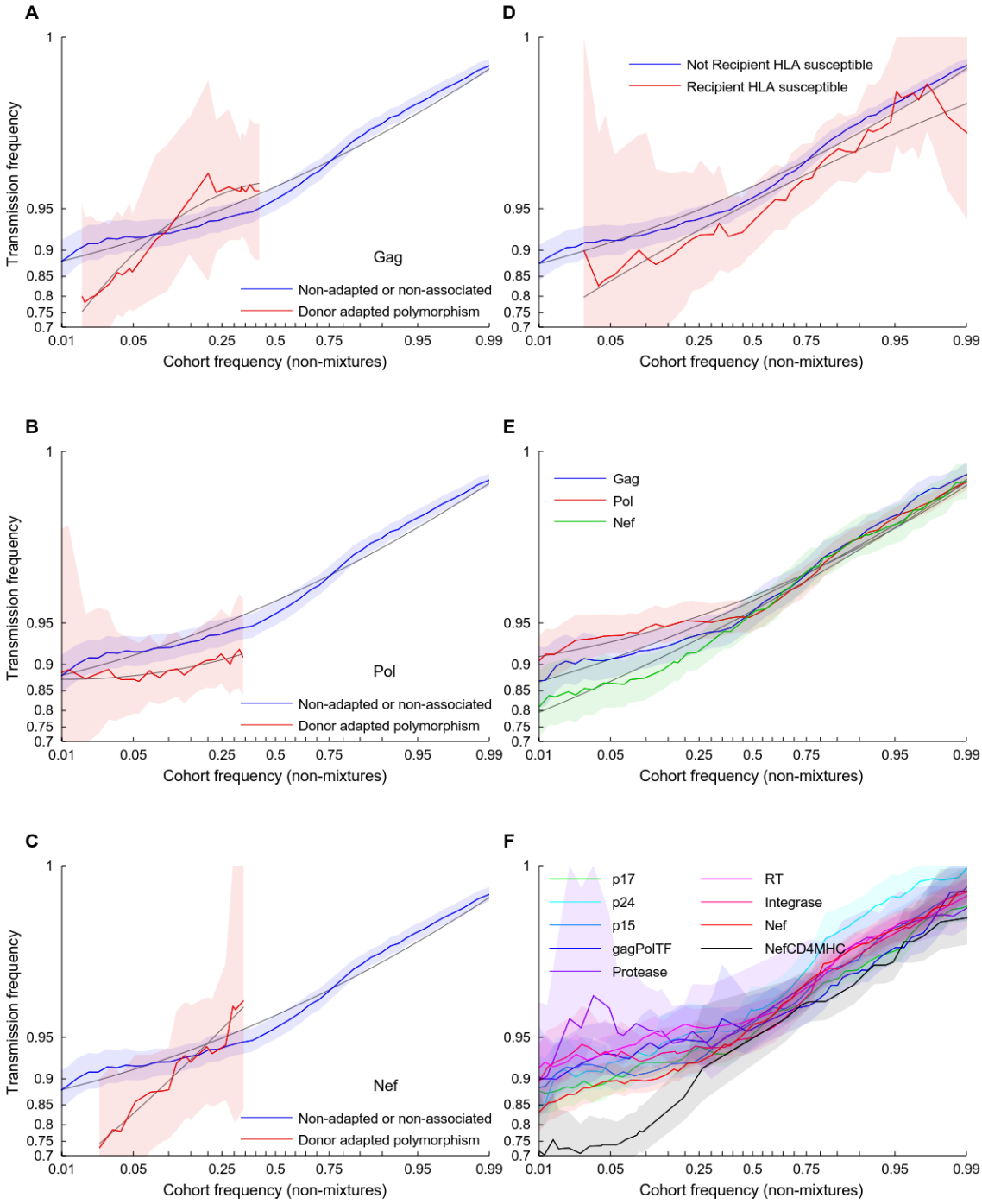

Fig. S2. Additional features that impact selection bias.

(**A-C**) Selection bias against transmission of variants that are consistent with escape from donor HLA alleles in (A) Gag, (B) Pol, and (C) Nef. (**D**) Residues that are susceptible to recipient HLA alleles—meaning they represent an un-escaped amino acid residue that is linked to at least one recipient HLA allele—are less likely to be transmitted. However, because transmission is defined as differences between recipient and donor sequences, as

measured a median of 46 days after transmission, these curves could represent rapid escape in the recipient. (**E**) Differences among proteins Gag, Pol and Nef, or (**F**) among protein domains. Although these differences were significant (see Table 2), no differences were observed when correcting for donor quasispecies frequency among the 5 couples for whom deep sequencing was available (Table 1), suggesting that these protein-specific difference may primarily result from differences in mean quasispecies frequencies of variants for these proteins. Nevertheless, these protein domains are included as covariates in all multivariable models to correct for confounding. Nef functional CD4 and MHC downregulation domains are taken from (*49*).

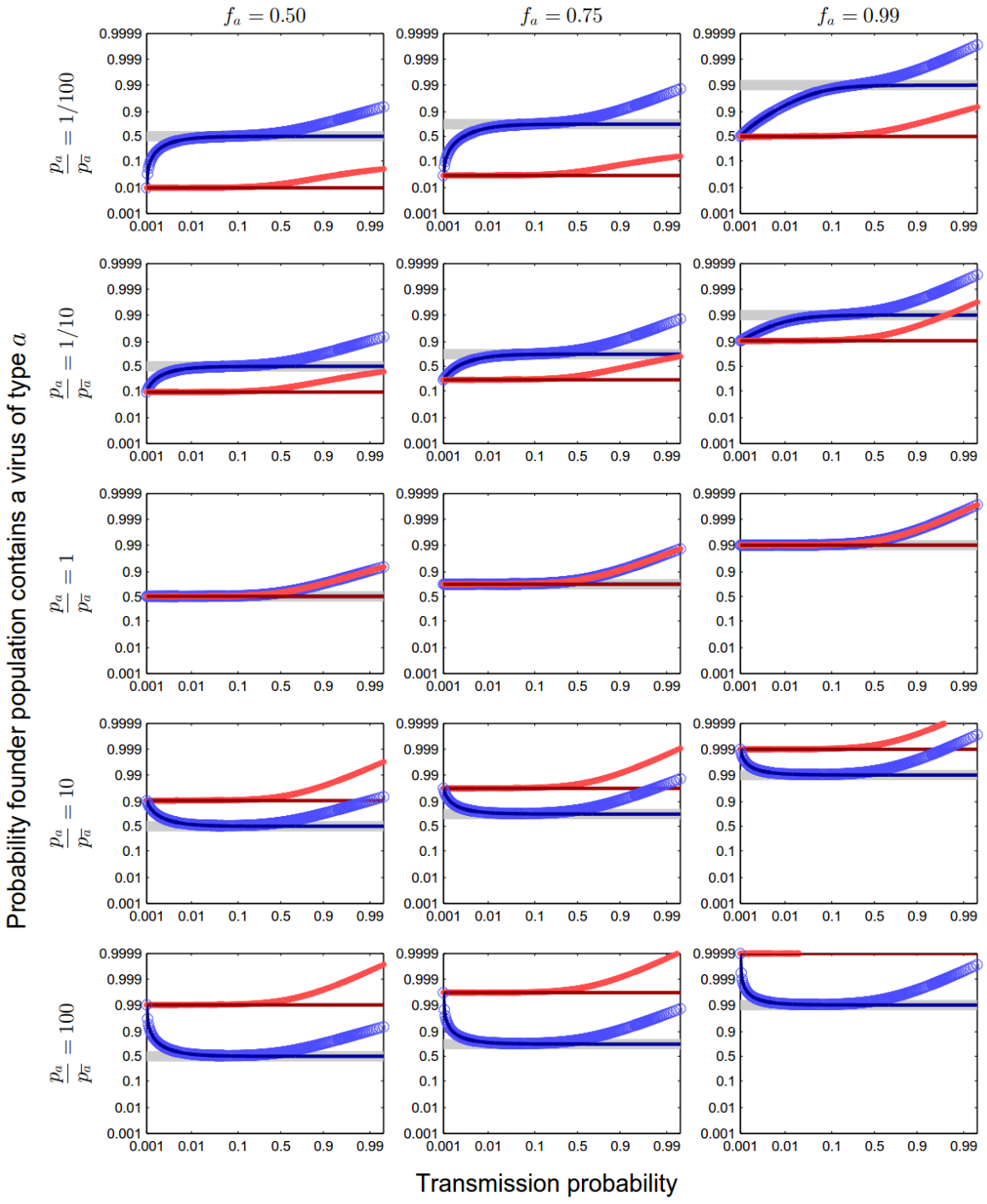

Fig. S3. Simulation of selection bias versus transmission probability.

The exact binomial probability mass function was used to explore the relationship between the probability of transmission, r, and the conditional probability that the transmitted founder virus population contains at least one virus of type a ($r_{a|r}$). For a range of 5 bias values ($p_a/p_{\bar{a}}$) and a range of donor quasispecies frequencies for a (f_a),

we plotted the conditional transmission probability of a as a function of the overall transmission probability r. For each plot, we set the donor viral population size to $n = 1000$, then solved for p_a to achieve a transmission probability of 0.001, satisfying bias, f_a, and n. We then increased the rate of transmission r, either by increasing the overall donor population size, n (red dots), or by increasing p for all viruses by adding a constant c to both p_a and $p_{\overline{a}}$ (blue circles). The red and blue solid lines indicate the predicted conditional transmission probability of a, as estimated by the approximation in Eq. 3. A reduction in selection bias is here visualized as the convergence of the conditional transmission probability toward f_a (gray line).

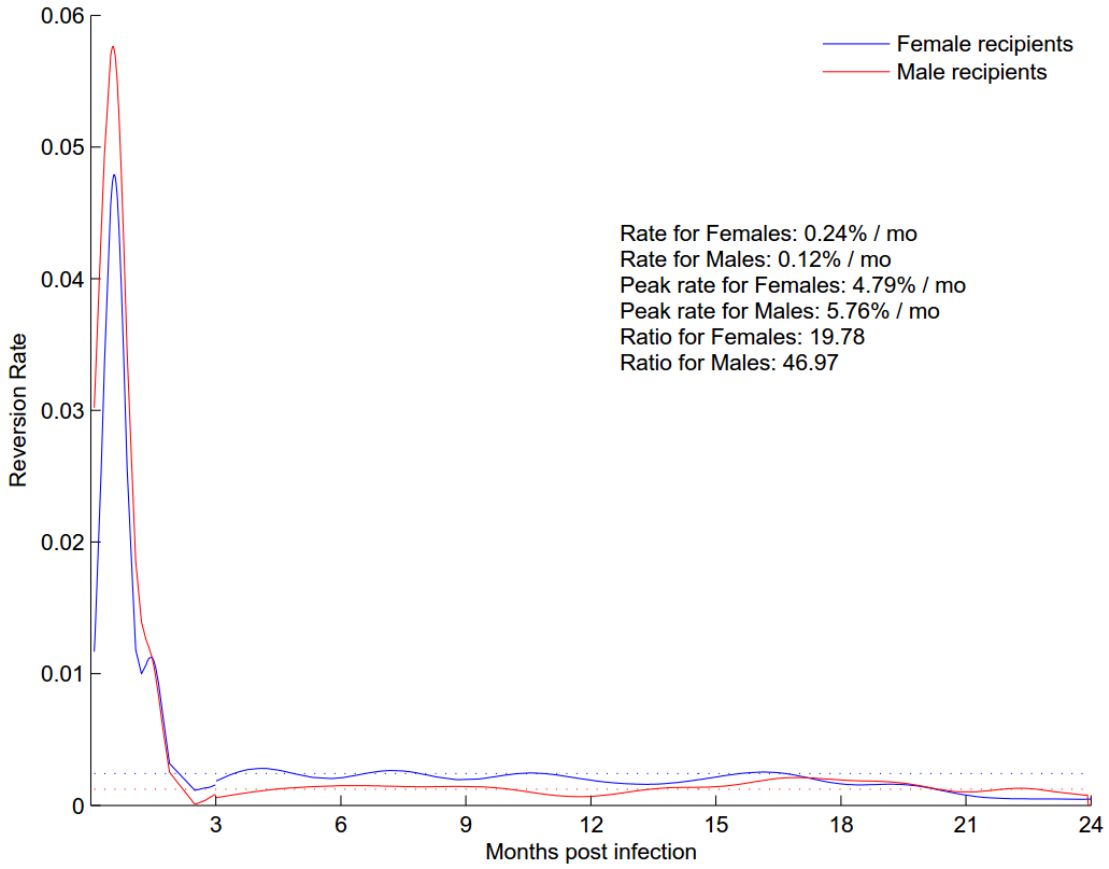

Fig. S4. Empirical reversion rates.

Empirical reversion rates of donor polymorphisms to non-mixture consensus were estimated using a kernel smoothing function, as implemented in the Matlab statistics package, using a Gaussian kernel with widths of 1 week and 1 month. The plot shows the curves with 1 week smoothing for <3mo and 1 month smoothing for >3mo (the larger smoothing window accommodates the sparser sampling times). Dotted lines show the mean reversion rates in the 3-12 month interval. Reversion rates are an order of magnitude higher in the first three months of infection compared to the following 18 months; steady state reversion rates are lower in males compared to females, whereas initial reversion rates are higher in males compared to females. These data are thus consistent with an initial selection bias and are not likely artifacts of early reversion, as further supported by the ability to estimate the odds of transmission of viruses and virus populations (Fig. 5). Compare to Fig. 4, which shows cumulative reversion. Note that Fig. 4 measures reversion times relative to the first available sample date in the recipient; here, reversion times are measured relative to the estimated date of infection.

Table S1. Clinical characteristics of the cohort.

	Transmitting	Non-Transmitting
N	137	181
Male (%)	62 (45%)	87 (48%)
Male recipient* GUI (%) [missing]	17 (29%) [3]	10 (12%) [1]
Female recipient GUI (%) [missing]	27 (38%) [3]	15 (16%) [2]
Male donor† log_{10} VL, median [IQR‡]	5.2 [4.7,5.7]	5.0 [4.3,5.3]
Female donor log_{10} VL, median [IQR]	4.8 [4.3,5.3]	4.3 [3.6,4.9]
ETI§, median [IQR]	46.0 [42.0,60.5]	

*In the case of non-transmitting couples, the "recipient" refers to the seronegative partner. †In the case of non-transmitting couples, the "donor" refers to the seropositive partner. ‡Interquartile range. §Estimated time between infection and first available sample.

Table S2. Reversion of donor polymorphisms transmitted to recipients

Feature	Ln(HR)*	*P* value†	Transmission‡	
Cohort frequency§	-0.28	0.016	+	
# Covarying sites	-0.10	0.031	+	
Donor escape	0.99	0.003	−	Viral fitness features**
Structural frequency§	0.01	0.496	+	
Donor $\log_{10}$ VL	-0.16	0.131	+	
Is male-to-female	0.58	0.016	+	Recipient susceptibility
Recipient is GUI male	0.17	0.406	+	features††
Is escape to consensus¶	1.45	0.004		
p17	-0.16	0.315		
p24	0.11	0.409		
Protease	-1.92	0.196		
Reverse transcriptase	-1.42	3.1×10^{-6}		
Integrase	-1.77	0.215		
Nef CD4/MHC domains	1.40	0.207		

*The hazard ratio of reversion from polymorphism to consensus, for sites in which a polymorphism was present in both the donor and recipient, were estimated using a Cox proportional hazards model. Only sites with available protein structures were used in the model; all sites were used in Fig. 4. †*P*-values were estimated using a multilevel bootstrap (1000 replicates) to estimate the standard error for each parameter. ‡The effect of the feature on odds of transmission (Table 2) is indicated: +, the feature generally increases odds of transmission; −, the feature generally decreases the odds of transmission. §Because we are tracking reversion to consensus, and not any mutation away from the polymorphism, observed cohort and predicted structure frequencies are here represented as the negative standardized log-odds of the respective measure for the cohort consensus at that site. ¶A binary variable indicating whether a mutation to consensus is consistent with escape from recipient HLA alleles, and thus may more likely represent immune escape than reversion. **Viral fitness features are expected to elicit opposite effects on transmission and reversion: amino acids with high odds of transmission will have low rates of reversion and vice versa. ††Recipient susceptibility features are expected to elicit concordant effects on transmission and reversion: individuals who have low selection bias will have high overall odds of transmitting the dominant donor variant; those variants will in turn revert faster because they on average have lower fitness.

Table S3. Transmission index of the seroprevalent partner is predictive of transmission

Feature	Ln(OR)*	*P* value
Offset	0.64	0.031
Transmission index†	1.28	0.047
Is male-to-female	1.11	0.705
Donor‡ $\log_{10}$ VL (M2F)§	1.47	0.031
Donor $\log_{10}$ VL (F2M)	2.18	4.4×10^{-4}
Recipient¶ has GUI (M2F)	1.00	0.986
Recipient has GUI (F2M)	3.41	0.010

*Model was fit using logistic regression. Dependent variable was whether the seroprevalent individual had transmitted to their partner. Compare to Fig. 5C. †Transmission index is standardized (zero mean, unit variance) for comparison purposes. ‡Or the seropositive partner in the case of NYT couples. §Donor VL and recipient GUI were given separate parameters for male-to-female (M2F) and female-to-male (F2M) couples. ¶Or the seronegative partner in the case of NYT couples.

Table S4. HLA associations, covariation associations and structural energy estimates (xls).